NASA TECHNICAL NOTE

NASA TN D-7971

NASA TN D-7971

EFFECT OF EXTERNAL DISTURBANCES AND DATA RATE ON THE RESPONSE OF AN AUTOMATIC LANDING SYSTEM CAPABLE OF CURVED TRAJECTORIES

Windsor L. Sherman

Langley Research Center
Hampton, Va. 23665

NATIONAL AERONAUTICS AND SPACE ADMINISTRATION • WASHINGTON, D. C. • SEPTEMBER 1975

1. Report No.	2. Government Accession No.	3. Recipient's Catalog No.
NASA TN D-7971		

4. Title and Subtitle	5. Report Date
EFFECT OF EXTERNAL DISTURBANCES AND DATA RATE ON THE RESPONSE OF AN AUTOMATIC LANDING SYSTEM CAPABLE OF CURVED TRAJECTORIES	September 1975
	6. Performing Organization Code

7. Author(s)	8. Performing Organization Report No.
Windsor L. Sherman	L-10040
	10. Work Unit No.
9. Performing Organization Name and Address	505-06-93-04
NASA Langley Research Center Hampton, Va. 23665	11. Contract or Grant No.
	13. Type of Report and Period Covered
12. Sponsoring Agency Name and Address	Technical Note
National Aeronautics and Space Administration Washington, D.C. 20546	14. Sponsoring Agency Code

15. Supplementary Notes

16. Abstract

The effects of steady wind, turbulence, data sample rate, and control-actuator natural frequency on the response of a possible automatic landing system described in NASA TN D-7611 have been investigated in a nonstatistical study. The results indicate that the system, which interfaces with the microwave landing system, functions well in winds and turbulence as long as the guidance law contains proper compensation for wind. The system response was satisfactory down to five data samples per second, which makes the system compatible with the microwave landing system. No adverse effects were observed when actuator natural frequency was lowered. For limiting cases, those cases where the roll angle goes to zero just as the airplane touches down, the basic method for computing the turn-algorithm gains proved unsatisfactory and unacceptable landings resulted. Revised computation methods gave turn-algorithm gains that resulted in acceptable landings. The gains provided by the new method also improved the touchdown conditions for acceptable landings over those obtained when the gains were determined by the old method.

17. Key Words (Suggested by Author(s))	18. Distribution Statement
Guidance Terminal area Landing	Unclassified – Unlimited Subject Category 04

19. Security Classif. (of this report)	20. Security Classif. (of this page)	21. No. of Pages	22. Price*
Unclassified	Unclassified	45	$3.75

*For sale by the National Technical Information Service, Springfield, Virginia 22161

EFFECT OF EXTERNAL DISTURBANCES AND DATA RATE ON THE RESPONSE OF AN AUTOMATIC LANDING SYSTEM CAPABLE OF CURVED TRAJECTORIES

Windsor L. Sherman
Langley Research Center

SUMMARY

The automatic landing system described in NASA TN D-7611 is capable of guiding a large transport airplane on curved decelerating trajectories to a landing on the airport runway. The system which takes over when the airplane is close in, 6000 m or less from the landing point, will, for the acquisition of guidance data, interface with the microwave landing system. A nonstatistical study has been made of the effect of wind, shear, turbulence, data sample, and control-actuator natural frequency on the response of the system. The results indicate that the system functions well in the presence of wind shears and turbulence. However, for steady wind the guidance laws, particularly the turn algorithm, must contain proper compensation for the effect of wind. The system had satisfactory response for data sample rates down to five samples per second and control-actuator natural frequencies of 5 Hz.

In limiting cases, those cases where the roll angle reaches zero as the airplane touches down, the gains in the turn algorithm computed by the methods given in NASA TN D-7611 produced unsatisfactory landings when winds and turbulence were included. A revised method for determining the turn-algorithm gains, presented herein, computes turn-algorithm gains that give satisfactory landings in the limiting cases. The use of gains determined by the methods in nonlimiting cases also improved the system response.

INTRODUCTION

Reference 1 presents the results of a study of a possible automatic landing system in a bland environment. The system studied is capable of guiding large jet transport-type aircraft over steep, curved decelerating trajectories over the portion of the landing operation that occurs just before touchdown. It takes over when the airplane is 6000 m or less from the landing point. The data requirements of the automatic landing system are compatible with the data output of the microwave landing system (MLS). This report extends the results presented in reference 1 to a nonbland environment. The effects of steady

wind, wind shear, random turbulence, data sample rate, and control-actuator natural frequency on the response of the airplane and system are shown. In the case of wind shear, the heading and/or the magnitude of the shear was dependent on altitude. In addition to the overall response study, the effect of initial conditions, position, altitude, and environmental conditions on the gains in the turn algorithm was studied. The present study, which is analytical in nature, was made on a large digital computer for the airborne automatic landing systems described in reference 1.

Ideally, the description of automatic landing system performance in a nonbland environment would be a statistical study involving multiple landings at various initial conditions so that rms errors could be determined. However, such a study involves rather complete knowledge of the system hardware characteristics as well as the specification of the external disturbances. In addition, a study of this type consumes vast amounts of computer time. Inasmuch as the hardware for the autoland system described in NASA TN D-7611 is not known and in order to conserve computer time, typical initial conditions including those at the limit of the system performances were studied on a nonstatistical basis. The results obtained, while not suitable for the determination of operational limitations, demonstrate the response of the system for various data sample rates and atmospheric disturbances, and show the effect of the initial condition on turn-algorithm gains together with a method for determining these gains.

SYMBOLS

The International System of Units (SI) is used throughout this paper. All angles are measured in radians. The coordinate systems referred to are discussed in appendix A.

B_{AA} radar azimuth angle in R_{jp} coordinates

B_{AC} desired radar azimuth angle in R_{jp} coordinates

C_{l_β} rolling-moment coefficient due to sideslip

H altitude

K desired angle between runway centerline and velocity vector at point B of figure 9

k_1 variable gain for the pseudo-radar azimuth angle error of the turn-control algorithm

k_2 variable gain for the total error used to determine roll command

k_3 = 0.3

k_4 gain used in computation of k_2, may be variable

q pitch rate

R_H projection of range vector in the z_1,z_2 plane

R_{jp} special radar coordinates used in calculation of k_1

R_{z_j} radar range components in z_j coordinates

U_G component of ground speed in y_1 direction

U_{wp} windspeed along R_{1p} axis evaluated at point A only

u_w windspeed along η_1-axis

V airplane speed

V_{wp} windspeed evaluated at point B only

v_w windspeed along η_2-axis

w_w windspeed along η_3-axis

w_{z_j} vertical speed in z_j coordinates

x_j radar coordinates

y_j airplane coordinates referred to principal body axes

z_j quasi-inertial coordinates

α angle of attack

β	sideslip angle
$\dot{\beta}$	sideslip angular rate, rad/sec
γ	flight-path angle
δ_a	aileron deflection
δ_r	rudder deflection
ζ_j	runway coordinates, referred to the desired landing point
η_j	inertial coordinates, translate with airplane
θ	pitch angle
θ_{AA}	radar azimuth angle in z_j coordinate
θ_{AC}	desired radar azimuth angle in z_j coordinate
θ_{AW}	wind correction angle
θ_{AAV}	radar azimuth angle in z_j coordinates referred to velocity vector
θ_{ACV}	desired radar azimuth angle in z_j coordinates referred to velocity vector
φ	roll angle
ψ	heading angle, airplane centerline
$\psi_r = 0$	heading angle of runway
ψ_v	heading angle of velocity vector
ψ_4, ψ_5	special heading angles used to determine k_1
$\overline{\psi}_c$	dummy yaw angle used in determination of k_1

Subscripts:

c command

i initial

j coordinate index, j = 1, 2, 3

A dot over a variable indicates differentiation with respect to time.

THE AUTOMATIC LANDING SYSTEM

The automatic landing system used in this study was fully described in reference 1. Briefly, data from an inertial table and either an airborne radar or the microwave landing system are processed in airborne computers to obtain guidance signals that direct the airplane along steep, curved approaches to the landing point. A moderate speed change, about 5 m/sec, was accomplished during the landing maneuver. The system operates during final approach and landing, assuming control of the airplane between 3000 m and 6000 m from the landing point. No major changes were made in the system as a result of the introduction of cross winds, turbulence, and sample rate. However, some modification of the heading angle and radar-azimuth-angle feedback were required to handle cross winds. In the presence of head winds, a change to the flare computer also was needed in order to insure that the airplane had the proper attitude angle at touchdown. These changes will be discussed when the appropriate results are presented. The block diagram of the autoland system with the changes found necessary for atmospheric disturbance is presented in figure 1.

The airplane that was modeled for this study was a large four-engined jet transport that had a mass of 90 719 kg. Complete data for the airplane are given in reference 1.

Disturbances Used

Steady winds with and without shear and turbulence were introduced as atmospheric (external) disturbances. In the case of steady wind, the wind was always considered to be parallel to the ground plane. Shear was introduced on the steady wind by two methods: (1) a magnitude change with altitude and (2) a direction change with altitude, which is referred to rotation. The magnitude changed at the rate of -0.048 m/sec per meter, from a windspeed of -25.80 m/sec at a 540-m altitude, and the rotation was 0.0058 rad/m.

The turbulence used in this study was based on a random-number program, the output of which is a normal distribution of random numbers between ± 1.0. As long as the initialization is not changed, the same set of random numbers is generated. The random

numbers generated by the program were used to generate an acceleration which was integrated to give a speed. The turbulence was generated in inertial coordinates, the η_j-system, and transformed into airplane body axes. A separate random-number generator with different initialization was used for each of the η_j-axes. Three levels of turbulence, mild, medium, and strong, were generated. The rms gust speed and the maximum gust speed for these three levels of turbulence are given in table I. Because the initialization of the random-number program was not changed during the course of the investigation, the turbulence repeated from run to run. Typical time histories of the medium turbulence are shown in figure 2. As can be seen from the time history, the turbulence consists of continuous gusts of relatively high intensity whereas atmospheric turbulence generally consists of brief periods of large gusts separated by periods of relative calm. A so-called patchy turbulence was obtained by using the output of one of the random-number generators to control the intensity of the gusts along the three η_j-axes. This produced a turbulence (see fig. 2) time history (labeled patchy) that more closely resembles atmospheric conditions than does the unmodified medium turbulence. The rms gust speed and the maximum gust speed are given in table I. During the study of the effect of turbulence on the system response all of the turbulences listed in table I were used. However, when combined with other effects, such as steady wind, either the medium or patchy types of turbulence were used.

In addition to the external disturbances, the sample rate (the number of times per sec that the continuous output of the guidance computers was read to obtain new values of φ_c and q_c) and the control-actuator natural frequency were varied. Five sample rates between 1000 samples per second and 5 samples per second were used. The control actuators programed for the autoland system were considered typical of a modern commercial jet airplane and had a natural frequency of 30 Hz. Natural frequencies as low as 5 Hz were used to determine the effect of varying this parameter on the system response.

Acceptable Touchdown Conditions

In the investigation reported herein it was assumed that the landing was taking place on a runway 3000 m long and 50 m wide. The desired touchdown point was on the centerline 100 m from the end of the runway. The values of φ, ψ, ζ_1, ζ_2, and γ, because of the reference used, indicate the errors from the ideal touchdown condition in which all these variables would have a value of zero. In this study, for the purpose of determining if a landing was satisfactory, an arbitrary set of conditions was established. If a landing fitted within the following limits, it was said to be satisfactory:

$\varphi = \pm 0.06$ rad

$\psi = \pm 0.01$ rad (except for steady winds)

$\zeta_1 = +500$ m

$\zeta_2 = \pm 10$ m (based on airplane model used in study)

$0 > \gamma \geqq -1.98 \times 10^{-2}$ rad

$0 < w_{z_j} \leqq 1.0$ m/sec

$0.017 \leqq \theta \leqq 0.061$ rad

The heading angle ψ reported in the tables is the heading of the airplane centerline with respect to the runway. The autoland system controls the pointing of the velocity vector, so in the presence of wind the reported heading angle is that which is required to direct the resultant ground-speed vector down the runway centerline. This approach to control minimizes speed perpendicular to the runway centerline. As the heading angle is a function of windspeed and direction, no real tolerance criterion is possible. However, the values of ψ given in table II for cases with wind place the velocity along the centerline within reasonable limits.

RESULTS AND DISCUSSION

The results obtained in this study can be divided roughly into the effect of wind condition and the effect of system conditions. Table II summarizes some of the results obtained in this study. Data are given for two important points in the landing maneuver, the start of the flare and the actual touchdown. The nominal point at which the flare is started is an altitude of 20 m. For the data given in table II and all tables that follow, the start of flare occurs in a narrow band about this nominal altitude, usually within ±10 percent. Case 1 in table II is the data for the autoland system described in reference 1. There were no disturbances in the model when these data were obtained. Because the results presented in reference 1 showed that if the gain k_1 was set correctly, the response of the system was not initial-condition dependent, only one initial condition was studied in detail, the one given in table II.

Effect of Turbulence

Cases 2 to 4 of table II show the effect of turbulence on the autoland system. An inspection of the ground and altitude tracks showed that there was little effect on them from the turbulence. The touchdown conditions with the exception of θ and w_{z_j} were, in general, acceptable.

The principal effect of turbulence was on the motion of the airplane itself. The effect on the airplane can be seen by comparing time histories of aircraft motion during a typical landing maneuver presented in figure 3. None of the motions presented appear too drastic and, as can be seen, the patchy turbulence produces slightly less effect than the medium turbulence. It should be emphasized that the autoland system used in the turbulence studies was the same system described in reference 1. No gains or other changes were made to the system. In general, the turbulence had no important effect on the ability of the system to execute a landing. During the remainder of the study when turbulence was used, it was the medium or patchy turbulence. The light turbulence had no effect on the system. The autoland system was able to control the airplane in the heavy turbulence; this was considered an extreme case because of the high gust speeds and high touchdown speed.

Steady Winds

Steady winds with speeds of -25.80 m/sec and 14.007 m/sec were used at various angles to the runway centerline between 0 and $\pi/2$. The ground tracks for the basic system (case 1) and the basic system with wind (cases 7 and 9) are shown in figure 4. The windspeed was -25.80 m/sec at $\pi/4$ rad to the runway centerline. With the wind present the ground track deteriorated as shown in figure 4 and touchdown conditions were not acceptable (see case 7, table II). The altitude track was also unacceptable. This deterioration was due to the fact that the guidance system basically controls the direction of the inertial velocity vector but the controlling parameters ψ and θ_{AA} are referenced to the airplane centerline.

The linear velocities $\dot{R}_{Z_1}$ and $\dot{R}_{Z_2}$ along the R_{Z_j}-axes were used to determine a wind correction angle θ_{AW} which is given by the following expression:

$$\theta_{AW} = \tan^{-1}\left(\frac{\dot{R}_{Z_2}}{\dot{R}_{Z_1}}\right) \tag{1}$$

The angle θ_{AW} was combined with the heading angle of the airplane ψ to obtain the heading angle of the velocity vector $\left(\psi_V = \psi + \theta_{AW}\right)$. In addition, through the use of this angle, R_{Z_1} and R_{Z_2} were transformed so that R_{Z_1} was along the velocity vector and R_{Z_2} perpendicular to it. The transformed values of R_{Z_1} and R_{Z_2} which are R_{1p} and R_{2p} were used to compute two new radar angles θ_{ACV} and θ_{AAV} that are referenced to the velocity vector. These new angles were used in the turn algorithm to determine φ_c. The modified equation for φ_c is

$$\varphi_c = k_2\left[\psi_c - \psi_V - k_3\dot{\psi} + k_1\left(\theta_{ACV} - \theta_{AAV}\right)\right] \tag{2}$$

This change of reference from the centerline to the velocity vector restores the accuracy of the autoland system (see case 9 in fig. 4). Cases 8 to 11 of table II summarize the

results obtained for steady winds and a comparison of the ground tracks is presented in figure 5. No changes in the letdown guidance were required and there were no effects on the altitude tracks.

The changes to the turn algorithm, summarized in equation (2), introduce wind and turbulence information into the determination of the turn commands. Cases 5 and 6 of table II were run in order to determine if turbulence affected the modified turn-control system. The data presented in the table for these cases indicate no effect on the system response. There were no significant changes in the ground and altitude tracks for these cases.

Two additional control changes were introduced to improve control with steady wind. These were $\dot{\beta}$, β, and δ_r feedbacks to the ailerons and a change in the flare computer. The former, which coordinates the turns, will be discussed first. Under some conditions of sideslip, the rolling produced by C_{l_β} is sufficient to cause the airplane to roll in the wrong direction. By feeding back $\dot{\beta}$, β, and δ_r to the aileron the undesired rolling moments were canceled. The commands from the guidance then modify the corrective δ_a to obtain the desired roll angle. Because the correction is dependent on β the correction is self-canceling as it approaches zero and as β approaches zero. This type of correction is not considered a mandatory part of the autoland system as the necessity for it depends on the aerodynamics of the particular airplane. The details of the change are shown in the block diagram in figure 1. The second change was included when an inspection of the touchdown conditions showed that the flare routine was not pitching the airplane sufficiently to insure a safe landing. A nonstandard procedure was adopted to obtain the desired pitch angle. The flap controls were modified so that the flaps were retracted until the airplane reached a pitch angle of 0.052 rad, a pitch angle that gives a reasonable pitch attitude at touchdown. The retraction was started at the time the flare was started.

In addition to steady winds, vertical wind shears and winds that changed directions were used. The introduction of these wind conditions did not cause the system to abort landings (see cases 12 to 14 of table II), nor did the airplane and system response (i.e., ground and altitude tracks) deteriorate.

When the wind is not directly along the runway, the airplane is flown so that the resulting velocity vector points in the correct direction; thus as the airplane approaches the runway, it is yawed, or crabbed, with respect to the runway centerline. Much has been done on the decrab maneuvers, that is, the alinement of the airplane and runway centerlines just before touchdown. Reference 2 reports a typical decrab-maneuver study for transport-type aircraft. The results given in reference 2 indicate that a decrab maneuver is feasible and that the systems used could be incorporated in the automatic landing system of this study. For these reasons no extensive study of the decrab maneuver was made; however,

enough work was done to establish that conditions at flare initiation and touchdown would make it feasible to incorporate a decrab maneuver.

The next logical step was to combine the steady winds and the turbulence. Ground and altitude tracks are shown in figure 6 for medium turbulence and a steady wind of -25.80 m/sec; this is case 15 of table II. As can be seen by a comparison of figures 5 and 7 the combined wind and turbulence caused little change in the tracks. The airplane responses were changed very little from those given in figure 3 for the medium turbulence. Both the medium and patchy turbulence were used in these runs; neither caused unsatisfactory results. Case 16 of table II combines all types of wind effect that have been used in this study. As can be seen, this combination did not have an adverse effect on either the touchdown conditions or the ground and altitude tracks.

Sample Rate

In the sample-rate studies it was assumed that the outputs of the angle and distance sensors were continuous and that the guidance computers used a finite number of samples of data per second for determining the guidance commands. Sample rates of 1000, 100, 50, 10, and 5 samples per second were used. The data sample rate was also the refresh rate for guidance commands. If 10 samples of data were taken per second, the guidance computer output per second was 10 discrete commands; one for each sample of data. The sample-rate tests were run with medium turbulence and are recorded as cases 5 and 17 to 20 of table II; case 5 is the basic case.

Data for these cases, presented in table II, show that there was little change in lateral variables with sample at the start of flare and the touchdown conditions were within acceptable limits. Ground tracks for case 5 (1000 samples per second) and case 20 (5 samples per second) are shown in figure 7. As can be seen, there are only small differences in the ground tracks of these extreme cases. Inspection of the results of the vertical mode indicated that up to the initiation of the flare the results were similar to those for the horizontal control. Conditions at the start of flare indicated that an acceptable flare could be performed. However, at touchdown the only variable that at all times was within acceptable limits was ζ_1. The vertical velocity at touchdown increased from 4.48×10^{-1} m/sec for 1000 samples per second to 2.30 m/sec for 5 samples per second, which is unacceptable. Oddly enough the pitch angle at touchdown changed from an unacceptable value of -6.46×10^{-2} at 1000 samples per second, to an acceptable value of 3.92×10^{-2} at 5 samples per second. The increase in the vertical touchdown speed w_{z_j} is accounted for by a failure of γ to decrease toward zero, as the sample rate decreased. Because $|\gamma|$ increased with decreasing sample rate, a refresh rate between 50 and 100 commands per second is indicated. The most practical way to accomplish this is to add a predictor to the flare computer so that commands between data samples can be generated.

Case 21 of table II combines the steady wind of -25.80 m/sec with the medium turbulence at 10 samples per second. The flare conditions for this indicate a good touchdown can be achieved but, as with the other 1000-samples-rate cases, θ and w_{z_j} proved to be unacceptable.

The fact that no uncorrectable deterioration of the system occurred at 5 and 10 samples per second is most important, as these are the data rates for the MLS system in category II and III conditions (see ref. 3). Because of their relationship to the MLS, sample rates of 10 and 5 samples per second were used for further study. No increase in the command refresh rate was incorporated in the system.

Control-Actuator Natural Frequency

The control actuators modeled for the autoland system were representative of the control surface actuators of large modern transport aircraft. Because this type of actuator has a natural frequency of about 30 Hz and has damping ratios greater than one, a first-order representation for the actuator was used in the study. In order to gain some idea of the effect of actuator natural frequency on the system response, a run was made with actuators with a natural frequency of 5 Hz. The sample rate was 5 samples per second. The ground track for this case differed very little from that for case 20 (see fig. 7), and the altitude track was satisfactory to the start of the landing flare. The touchdown conditions are given in table II as case 22, and are satisfactory except for θ and w_{z_j}. These results were typical when the natural frequency of the three control-surface actuators was the same. However, if the natural frequency of each actuator was different the system response was much poorer than that for case 22. The worst response, which was not acceptable, occurred when the aileron and rudder actuators had the same natural frequency, and the natural frequency of the elevator actuator was lower than the others.

Discussion of Results Presented in Table II

In cases 1 to 22, when properly compensated for environmental conditions, the lateral (turn control) guidance was able to reduce the lateral displacement errors and heading-angle errors to acceptable values. The absolute value of the roll angle at touchdown was equal to or less than 5.35×10^{-2} rad which is within the acceptable limits. This was not the case in longitudinal guidance, as for 13 of 22 cases in table II either θ and/or w_{z_j} did not fall within acceptable limits. Of these 13 cases, there were 3 (cases 3, 19, and 20) where the value of only w_{z_j} was unacceptable. In cases 6, 12, 14, 15, 16, 17, and 18 all of the longitudinal touchdown conditions were satisfactory. The average values of three longitudinal parameters, the pitch angle θ, the flight-path angle γ, and the sink rate w_{z_j} were computed at the start of the flare and are

$\theta = -6.83 \times 10^{-2}$ rad

$\gamma = -5.48 \times 10^{-2}$ rad

$w_{z_j} = 4.023$ m/sec

In all cases where one or more of the longitudinal parameters did not meet the criterion for acceptable touchdown conditions, one or more of the parameters θ, γ, and w_{z_j} deviated from the above values at flare initiation. For instance, in case 1 where only w_{z_j} did not meet acceptable touchdown conditions, the sink rate at the start of the flare was 1.07 m/sec above the previously given average. This suggests that more precise control of the state conditions at the start of the flare would help to obtain acceptable touchdowns. One interesting point connected with the acceptable landings is that there is either no steady wind in the problem or a wind with a shear pattern that reduces the windspeed to zero at ground level. This implies that there is an effect of steady wind on system performance that has not been completely identified.

Limiting Initial Conditions

In reference 1 limiting initial conditions were defined as those cases in which the roll angle reached an acceptable value as the airplane touched down on the runway. One such case has the following initial conditions:

$\zeta_1 = -3000.0$ m

$\zeta_2 = -4000.0$ m

$H = 540$ m

$\psi_i = 0.0$

When this initial condition was used in reference 1 a satisfactory landing resulted. The results for the present case with a steady wind of -25.80 m/sec at $\pi/4$ rad to the runway centerline and patchy turbulence are given as case 23 of table III. All touchdown conditions were unacceptable and the conditions for θ, γ, and w_{z_j} at flare initiation differed greatly from the previously given average values at this point. The complete unacceptability of this case is borne out by the ground track (see fig. 8).

A rerun of this case without the steady winds showed large improvement in the touchdown conditions. This result again pointed to an effect on the system of a steady wind. Although the determination of the parameters in the lateral guidance had been changed to account for steady wind, the gains k_1 and k_2 were still being computed by the methods

given in reference 1. As was pointed out in reference 1, system performance is very sensitive to these gains and these gains are sensitive to initial conditions; therefore, the logical place to look for an uncorrected wind sensitivity was these gains.

The Gains k_1 and k_2

The gains k_1 and k_2 are used in the lateral-guidance turn algorithm (eq. (2)). The gain k_1 is recomputed whenever the direction of the turn is changed and the gain k_2 is continuously calculated as a function of the heading angle. For this method k_1 calculated at the beginning of the landing maneuver does not take atmospheric conditions into account; however, any subsequent calculation of k_1 does take these conditions into account. Therefore, it is the first calculation of k_1 for which a revision was made. The new method of calculating the initial value of k_1 was changed to consider winds. (See appendix B.) A comparison of the results for k_1 computed by the method of reference 1 (case 23) and that of appendix B when equation (B9) is used to calculate k_1 (case 25) is given in table III. Cases 24 and 26 show the effect of small changes, approximately 2.5 percent in the k_1 of case 25. The change of k_1 to 1.759 produced a set of satisfactory landing conditions. While the values of θ, γ, and w_{z_j} at flare initiation are not close to the previously given average values of these parameters for the acceptable cases of table II, they lie within the spread of the data of these cases. Increasing k_1 by approximately 2.5 percent produces a completely unacceptable landing, case 24. Decreasing k_1 by about the same amount improved the values of the parameters φ, ψ, and ζ_2; but the overshoot in the ζ_1 direction, about 800 m, may not be acceptable for short runways. Case 25 was adopted as a base case for the study of the effect of the gain k_2. Figure 8 compares the ground tracks for cases 23 and 25.

The Effect of Varying the Gain k_2

The gain k_2 appears in equation (2) as a multiplicative factor of the total error and converts this heading angle and position error to a bank-angle command. The gain k_2 is given by

$$k_2 = \frac{k_4}{k_1} e^{-|\psi_c - \psi_v|} \tag{3}$$

where k_4 is a constant. The only way to vary k_2 is to change k_4. These changes in k_4 are listed in table IV. However, because k_2 appears in equation (2), the changes are referred to as variations in k_2. The changes in k_2 do not affect k_1 so no values of k_1 are given. The values of k_1 are the same as corresponding cases of table III. Two basic cases were used for table IV: case 23 in which the landing was unsatisfactory, and case 25 in which the landing was satisfactory. An inspection of cases 23, 23a, 23b, and 23c shows that when k_1 was not correct, variations in k_2 did not improve the

landing conditions but actually shows further deterioration in some of the parameters such as the roll angle φ. However, when k_1 had a value that gave a satisfactory landing (case 25) changes in k_2 definitely affected the landing. When k_4 was decreased from 4.8 (case 25, table IV) to 4.4 (case 25a, table IV) all of the landing parameters improved, φ and ζ_2 were reduced by about an order of magnitude with smaller improvements in the overshoot in the ζ_1 direction, and there was a small improvement in the pitch attitude at touchdown. When k_4 was reduced still further to 4.0, the landing conditions moved back closer to those obtained when k_4 was equal to 4.8. Accordingly, a value of 4.4 was adopted for k_4. The values of θ, γ, and w_{z_j} at flare initiation did not match the average values of these parameters for the acceptable cases of table II and the only one that fell within the spread of the data was w_{z_j}. These results appear to indicate that correct values of k_1 and k_2 are the important factors in achieving a successful landing.

To this point the only value of ψ_i used in the study of the gains is 0.0. Other values of ψ_i were tried and it was found that a small correction to the gains k_1 and k_2 based on initial heading angle was required to obtain the best landing conditions over a wide range of ψ_i. The final equations used to compute k_1 and k_2 are equations (B10) and (B14) of appendix B.

Table V summarizes the conditions at the start of flare and at touchdown and ground tracks are shown in figure 9 when equations (B10) and (B14) were used to calculate k_1 and k_2. These results are for the following initial conditions:

$\zeta_1 = -6000$ m, $\zeta_2 = -4000$ m

H = 540 m, $\psi_i = 0.0, \pi/4, \pi/2$

$\zeta_1 = -3000$ m, $\zeta_2 = -4000$ m

H = 540 m, $\psi_i = 0.0, \pi/4, \pi/2$

with patchy turbulence and a steady wind of -25.80 m/sec at $\pi/4$ rad to the runway centerline. The sample frequency was 10 per second. The gains k_1 and k_2 which appear in the turn algorithm primarily affect the ground track of the airplane; however, because the flight-path command γ_c is determined in a plane that is perpendicular to the ground plane and passes through the start-of-flare point and the instantaneous position of the airplane, some effect of the lateral guidance can be expected on the letdown of the airplane. As can be seen from table V and figure 9, the lateral control is very good and the airplane is well alined with the runway before touchdown with very small roll angles and lateral displacements from the runway center. The body yaw angles indicate that the pointing of the velocity vector with respect to the runway centerline is also satisfactory. The

longitudinal touchdown conditions were not satisfactory with regard to pitch angle (cases 27a and 27b) which was too small; in case 27b, w_{z_j} is slightly high. Case 28c is also interesting. The pitch angle and w_{z_j} are both good although θ is a little high, the large discrepancy being the overshoot of the touchdown point. In this case, the overshoot is over 800 m but is still within the first third of the assumed 3000-m runway which is acceptable. A detailed study of the results indicated that the control system was functioning in the intended manner, that is, the flight-path angle was approaching zero and the airplane was pitching up to the proper touchdown attitude. This lack of proper performance in the flare region is in marked contrast to the performance of the longitudinal control system in the letdown prior to the flare. In this preflare region the letdown was well controlled with end conditions that should have permitted the execution of an acceptable flare.

The inconsistency of flare performance occurred not only in the results presented in this section, but in the results presented in the other sections of the paper. In addition to command refresh rate during the flare, analysis of the data indicates that the slowness of the speed control and/or the lack of coordination between the flight-path control system and speed control system may be the causes of the flare-touchdown problems. A better coordinated flare controller or a decoupled control system for the longitudinal mode which controls the flight path, pitch angle, and speed might help these problems. Research on a decoupled control system, steady-state decoupling only, for STOL aircraft (refs. 4 and 5) has shown this type of system to be highly effective for precise control of the longitudinal mode.

CONCLUDING REMARKS

An automatic landing system capable of guiding an airplane over steep, curved paths to a landing has been studied to determine the effect of wind, turbulence, data sample rate, and control-actuator natural frequency on the ability of the system to execute a landing. It was found that wind, including shears, and turbulence did not impair the ability of the autoland system to execute a landing. The gains in the turn algorithm, k_1 (variable gain for the pseudo-radar azimuth angle error of the turn-control algorithm) and k_2 (variable gain for the total error used to determine roll command), were critical factors in a successful landing and should be determined by the method presented in this paper. There were no observed effects of changing the control-actuator natural frequency as long as all three control actuators had the same natural frequency. Sample rates down to five samples per second were studied. At microwave-landing-system sample rates of 5 and 10 samples per second good system response was maintained and successful landings were executed.

The lateral response, alinement, and centering of the airplane with the runway were consistent and precise, as was the longitudinal response to the start of the flare. After the start of the flare there was a lack of consistency in the longitudinal response resulting

in unacceptable or marginal values of touchdown distance, pitch angle, flight-path angle, and vertical speed at touchdown. The most probable causes were a low command refresh rate in the flare, the slow response of the speed control, and a lack of coordination between the speed system and the flight-path control system. A steady-state decoupled control system, that controls speed as well as flight path, should be investigated as a longitudinal control system.

Langley Research Center
National Aeronautics and Space Administration
Hampton, Va. 23665
May 30, 1975

APPENDIX A

COORDINATE SYSTEMS USED IN STUDY

Five coordinate systems were used in the autoland system:

(1) inertial coordinates	η_j
(2) quasi-inertial coordinates	z_j
(3) airplane coordinates	y_j
(4) radar coordinates	x_j
(5) runway coordinates	ζ_j

Figure 10 shows these coordinate systems and their relationship for a typical landing situation. The subscript j in the symbol for the coordinates takes on the values 1, 2, or 3, the values denoting a specific axis. When $j = 1$, the axis corresponds to the x-axis of a usual x,y,z coordinate system. Similarly, $j = 2$ corresponds to the y-axis, and $j = 3$ the z-axis.

The inertial coordinates do not rotate and are forced to translate with the airplane. The η_1-axis has the same direction as the runway centerline. The quasi-inertial coordinates are rotated by the angle ψ, obtained by a positive rotation about the η_3-axis. The z_1-axis now points in the direction of flight. The airplane coordinates are related to the quasi-inertial system through the two additional angles θ, obtained by a position rotation about the z_2-axis, and ψ, obtained by a positive rotation about the y_1-axis.

The runway coordinates use the touchdown point as a fixed origin and the ζ_1 is positive toward the far end of the runway. These coordinates, except for $j = 3$, are the negative of the inertial system. This system is used only for the reporting of the results.

APPENDIX B

DISCUSSION OF THE GAINS k_1 AND k_2 THAT ARE USED IN THE TURN ALGORITHM

The basic equation in the turn algorithm (eq. (2)) determines the bank-angle command. Of the three gains in this equation k_1 and k_2 are the most important. These gains, through their influence on bank angles, influence the shape of the ground track and the letdown commands.

The Gain k_1

Figure 11 represents the ground track for an initial condition such as case 23 of table III. The points marked A and B in this figure are the points at which k_1 is calculated. The gain k_1 is calculated at point A so that the airplane will turn onto a heading that is approximately $\pi/2$ rad with respect to the runway and have zero bank angle when at point B. The second value of k_1 is calculated at point B to give good landing conditions at the touchdown point and to prevent the airplane from making a reverse turn at point B. Experience has shown that these two conditions are compatible and the condition applied is $\varphi_c = 0.0$ at point B. The basic modification required to the method given in reference 1 for the computation of k_1 at point A is the proper inclusion of the wind done in the following manner:

$$R_{1p} = R_{z_1} \cos (K - \psi) + R_{z_2} \sin (K - \psi) \tag{B1}$$

$$R_{2p} = -R_{z_1} \sin (K - \psi) + R_{z_2} \cos (K - \psi) \tag{B2}$$

$$U_{wp} = u_w \cos K + v_w \sin K \tag{B3}$$

$$V_{wp} = -u_w \sin K + v_w \cos K \tag{B4}$$

where K is a constant that is the angle between the runway centerline and the desired heading of the airplane at point B and u_w and v_w are the wind components along and perpendicular, respectively, to the runway centerline. The calculated parameters R_{1p}, R_{2p}, U_{wp}, and V_{wp} were used to determine ψ_4, ψ_5, and B_{AC} as follows:

$$\psi_4 = \tan^{-1}\left(\frac{V_{wp}}{U_G}\right) \tag{B5}$$

$$\psi_5 = K + \psi_4 \tag{B6}$$

$$B_{AA} = \tan^{-1}\left(\frac{R_{2p}}{R_{1p}}\right) - \psi_4 \tag{B7}$$

$$B_{AC} = \tan^{-1}\left[\frac{100.0}{\left(R_{1p}^3 + R_{2p}^2\right)^{1/2} \cos B_{AA}}\right] \tag{B8}$$

where U_G is the component of the ground speed in the y_1 direction. The parameters B_{AC}, B_{AA}, and ψ_5 were used to determine k_1 from the following equation:

$$k_1 = \left|\frac{\bar{\psi}_c - \psi_5}{B_{AC} - B_{AA}}\right| \tag{B9}$$

This value of k_1 proved adequate for an initial condition such as case 23 or case 1. However, when the initial heading angle is between 0.0 and $\pi/2$, a modification based on heading angle was required. The final equation for k_1 which is adequate for all ψ_i is

$$k_1 = \left|\frac{\bar{\psi}_c - \psi_5}{B_{AC} - B_{AA}}\right| - 0.09 \sin\left(2\psi_i\right) \tag{B10}$$

The value of k_1 determined by equation (B10) was used until the airplane reached point B in figure 11, at which point k_1 was recalculated. Point B was identified by the passage of the roll angle through zero, the actual condition being

if $(-0.002 \leq \varphi \leq 0.002)$ recalculate k_1

$$k_1 = \left|\frac{\psi_c - \psi_v - k_3\dot{\psi}}{\theta_{ACV} - \theta_{AAV}}\right| \tag{B11}$$

The value of k_1 determined by equation (B11) was used from point B until the airplane touched down.

The parameter K gives the desired heading angle between the runway centerline and the flight path at the point where k_1 is recalculated. The value assigned to K is $\pi/2$ and was used because it eliminates the possibility of singular conditions occurring in equations (B10) and (B11).

The program used for the computation of k_1 contained a lower limit on the value. That is, if the calculated k_1 was less than 1.483 for a left-turn approach or less than 1.524 for a right-turn approach, it was set to 1.483 or 1.524. Case 28a of table V was the only case of this study where k_1 passed below the limits. A study of case 28a showed

that better landings were obtained when the lower limit on the k_1 was dropped. Accordingly, the lower limits on k_1 have been dropped from the turn algorithm and the data given for case 28a of table V are without lower limits on k_1.

The work on the gain k_1 showed that the critical value is the one determined at point A of figure 11 by equation (B10). A correct value of k_1 at this point insures a correct value at point B and ensues a good landing.

The Calculation of Gain k_2

The gain k_2 is calculated from the equation

$$k_2 = \frac{k_4}{k_1} e^{-|\psi_c - \psi_v|} \tag{B12}$$

and effectively gives the radians of bank per radian of error. The expression for k_2 shows that the only way in which k_2 can be changed is to vary k_4.

The effect of varying k_4 on the touchdown conditions is presented in table IV and discussed in the subsection entitled "The Effect of Varying the Gain k_2." A sizable group of initial conditions were run and an analysis of the results showed that the proper value of k_4 could be calculated from

$$k_4 = 4.445 - 0.293\psi_i \tag{B13}$$

which makes the formulas for k_2

$$k_2 = \left(\frac{4.445 - 0.293\psi_i}{k_1}\right) e^{-|\psi_c - \psi|} \tag{B14}$$

Remarks on the Turn Algorithm

During the course of this investigation, several changes have been made to the turn algorithm as the result of wind disturbances and improved methods of determining the gains k_1 and k_2. These changes are summarized in the turn algorithm shown in figure 12. This turn algorithm is the one recommended for use with the autoland system described in reference 1. The improvement obtained through the use of this new algorithm is shown by a comparison of case 23 of table III $\left(k_4 = 4.4\right)$ with case 25a of table IV.

REFERENCES

1. Sherman, Windsor L.; and Winfrey, Sylvia W.: Preliminary Study of a Possible Automatic Landing System. NASA TN D-7611, 1974.

2. Bleeg, Robert; Hansen, R.; and Tisdale, H. F.: RSFS Control Law Development. Doc. No. D6-41552, Boeing Co., 1974.

3. Edwards, Jack W.: The National Microwave Landing System. IEEE NEREM. 73 Record, vol. 15, pt. 1, 1973, pp. 212-215.

4. Miller, G. Kimball, Jr.: Computer Program for Solving Gains Required for Steady-State Decoupling of Elements of Longitudinal Mode of an Airplane. NASA TM X-3020, 1974.

5. Miller, G. Kimball, Jr.; Deal, Perry L.; and Champine, Robert A.: Fixed-Base Simulation Study of Decoupled Controls During Approach and Landing of a STOL Transport Airplane. NASA TN D-7363, 1974.

TABLE I.- CHARACTERISTICS OF TURBULENCE USED IN STUDY

	rms gust speed, m/sec, along axis –			Maximum gust speed, m/sec, along axis –		
	η_1	η_2	η_3	η_1	η_2	η_3
Mild turbulence	0.163	0.173	0.185	±0.45	±0.45	±0.55
Medium turbulence	1.59	1.83	1.88	±4.5	±4.6	±5.5
Heavy turbulence	4.85	5.5	5.6	±9.3	±18.3	±16.4
Patchy turbulence	1.177	1.476	1.353	±5.86	±7.23	±9.73

TABLE II.- SUMMARY OF THE EFFECT OF WIND, TURBULENCE, SAMPLE RATE, AND CONTROL-ACTUATOR NATURAL FREQUENCY ON THE AUTOLAND SYSTEM

[Initial condition: ζ_1 = -6000 m; ζ_2 = -4000 m; H = 540 m; $\psi_i = \frac{\pi}{2}$; V_i = 77.12 to 102.92[a]]

Case no.	Wind conditions					System condition		Measuring point	Airplane states								
	Windspeed, m/sec	Direction, rad	Turbulence	Shear	Rotation	Sample rate	Average actuator N.F., Hz		φ, rad	ψ, rad	ζ_2, m	ζ_1, m	γ, rad	θ, rad	w_{z_j}, m/sec	Time, sec	V, m/sec
1 [b]	0.0	0.0	0.0	None	None	1000	30	Start of flare	3.82×10^{-3}	3.40×10^{-5}	-1.11	-3.14×10^{2}	-5.75×10^{-2}	-8.16×10^{-2}	4.16	116	72.38
								Touchdown	-9.41×10^{-4}	1.93×10^{-3}	-9.39×10^{-2}	2.84×10^{2}	-9.59×10^{-3}	-1.46×10^{-2}	6.71×10^{-1}	124	69.87
2 [b]	.0	.0	Light	None	None	1000	30	Start of flare	3.58×10^{-3}	3.23×10^{-4}	-1.06	-2.98×10^{2}	-5.90×10^{-2}	-8.58×10^{-2}	4.30	116	72.93
								Touchdown	-2.84×10^{-3}	8.76×10^{-4}	3.90×10^{-1}	2.65×10^{2}	-1.04×10^{-2}	-1.58×10^{-2}	7.32×10^{-1}	124	70.02
3 [b]	.0	.0	Medium	None	None	1000	30	Start of flare	3.03×10^{-3}	2.13×10^{-3}	-1.20	-3.202×10^{2}	-7.09×10^{-2}	-1.05×10^{-1}	5.09	115	71.84
								Touchdown	-1.3×10^{-2}	-9.62×10^{-4}	5.52	2.31×10^{1}	-1.83×10^{-2}	9.98×10^{-3}	1.29	120	70.93
4 [b]	.0	.0	Heavy	None	None	1000	30	Start of flare	7.80×10^{-3}	2.00×10^{-4}	-1.28	-3.31×10^{2}	-9.49×10^{-2}	-1.84×10^{-1}	1.52	115	83.21
								Touchdown	2.43×10^{-2}	-1.80×10^{-2}	7.82	7.39×10^{1}	-5.68×10^{-2}	-1.14×10^{-1}	4.79	118	84.36
5 [c]	.0	.0	Medium	None	None	1000	30	Start of flare	5.94×10^{-3}	-7.12×10^{-3}	-1.22	-2.49×10^{2}	-7.64×10^{-2}	-9.53×10^{-2}	5.52	116	72.31
								Touchdown	3.74×10^{-2}	-8.26×10^{-3}	-1.25	1.13×10^{2}	-6.29×10^{-3}	-6.48×10^{-3}	4.46×10^{-1}	122	71.08
6 [c,d]	.0	.0	Patchy	None	None	1000	30	Start of flare	1.69×10^{-2}	-1.09×10^{-2}	-2.80	-3.32×10^{2}	-4.52×10^{-2}	-9.95×10^{-2}	3.28	114	72.81
								Touchdown	-1.45×10^{-3}	-1.45×10^{-2}	-1.68	9.69×10^{1}	-6.72×10^{-3}	6.28×10^{-2}	4.94×10^{-1}	120	73.41
7 [b]	-25.80	$\pi/4$	None	None	None	1000	30	Start of flare	9.98×10^{-3}	3.13×10^{-1}	-1.15×10^{2}	-1.91×10^{2}	-2.62×10^{-2}	-1.06×10^{-1}	1.89	111	72.05
								Touchdown	3.07×10^{-1}	5.56×10^{-1}	1.20×10^{-2}	1.32×10^{3}	-1.15×10^{-2}	-1.02×10^{-1}	7.79×10^{-1}	133	67.55
8 [b]	-25.80	π	None	None	None	1000	30	Start of flare	-1.69×10^{-2}	8.62×10^{-3}	2.63	-2.77×10^{2}	-5.44×10^{-2}	-1.56×10^{-1}	3.98	121	73.11
								Touchdown	-9.65×10^{-3}	-9.64×10^{-3}	2.16	3.37×10^{2}	-8.18×10^{-3}	-1.15×10^{-1}	5.81×10^{-1}	130	71.06
9 [c,e]	-25.80	$\pi/4$	None	None	None	1000	30	Start of flare	-5.73×10^{-3}	1.99×10^{-1}	-4.21×10^{-1}	-2.92×10^{2}	-6.06×10^{-2}	-1.51×10^{-1}	4.45	103	73.55
								Touchdown	3.07×10^{-3}	1.97×10^{-1}	-3.08×10^{-1}	2.59×10^{2}	-9.74×10^{-3}	-1.04×10^{-1}	7.03×10^{-1}	110	72.15
10 [c,e]	-25.80	$\pi/2$	None	None	None	1000	30	Start of flare	1.02×10^{-2}	3.43×10^{-1}	-5.35	-3.10×10^{2}	-5.53×10^{-2}	-1.04×10^{-1}	4.07	106	73.64
								Touchdown	5.91×10^{-3}	3.50×10^{-1}	-1.42	3.23×10^{2}	-8.11×10^{-3}	-4.60×10^{-2}	5.78×10^{-1}	115	71.35
11 [c,e]	-14.007	$\pi/2$	None	None	None	1000	30	Start of flare	9.32×10^{-3}	1.93×10^{-1}	-3.52	-2.97×10^{2}	-5.62×10^{-2}	-8.71×10^{-2}	4.07	111	72.54
								Touchdown	5.35×10^{-3}	2.01×10^{-1}	-1.36	3.09×10^{2}	-8.54×10^{-3}	-2.37×10^{-2}	5.98×10^{-1}	120	70.05
12 [c,d,f]	-25.80	$\pi/4$	None	Yes	None	1000	30	Start of flare	-1.35×10^{-2}	2.43×10^{-2}	-1.22×10^{-2}	-2.88×10^{2}	-6.03×10^{-2}	-1.19×10^{-2}	4.55	100	75.46
								Touchdown	-7.32×10^{-3}	9.99×10^{-3}	-2.26	9.67×10^{1}	-8.87×10^{-3}	4.81×10^{-2}	6.59×10^{-1}	105	74.26
13 [c,d,e,g]	-25.80	- - -	None	None	Yes	1000	30	Start of flare	4.85×10^{-2}	4.85×10^{-2}	-8.84	-2.83×10^{2}	-5.84×10^{-2}	-1.65×10^{-2}	4.18	111	71.65
								Touchdown	5.57×10^{-2}	1.14×10^{-1}	-7.22	1.33×10^{2}	-1.38×10^{-2}	-1.79×10^{-2}	1.01	117	73.28
14 [c,d,f,g]	-25.80	- - -	None	Yes	Yes	1000	30	Start of flare	1.12×10^{-2}	1.30×10^{-3}	-2.59	-2.83×10^{2}	-5.88×10^{-2}	-1.08×10^{-2}	4.31	110	73.40
								Touchdown	8.48×10^{-4}	7.37×10^{-3}	-1.28	1.51×10^{2}	-7.93×10^{-3}	6.17×10^{-2}	5.80×10^{-1}	116	73.18
15 [c,d,e]	-25.80	$\pi/4$	Medium	None	None	1000	30	Start of flare	-9.69×10^{-3}	1.95×10^{-1}	3.23	-3.09×10^{2}	-4.40×10^{-2}	-1.51×10^{-2}	3.25	100	73.85
								Touchdown	3.46×10^{-3}	1.84×10^{-1}	2.04	2.29×10^{2}	-1.13×10^{-2}	2.51×10^{-3}	8.50×10^{-1}	107	75.54
16 [c,d,e,f,g]	-25.80	- - -	Medium	Yes	Yes	1000	30	Start of flare	-1.72×10^{-2}	-3.23×10^{-3}	6.10	-3.05×10^{2}	-4.47×10^{-2}	-8.01×10^{-2}	3.29	100	73.69
								Touchdown	7.39×10^{-3}	-1.22×10^{-2}	-1.71	4.80×10^{2}	-1.19×10^{-2}	1.18×10^{-1}	8.64×10^{-1}	111	72.65
17 [c,d,e]	.0	.0	Medium	None	None	100	30	Start of flare	-6.52×10^{-3}	-9.35×10^{-3}	-2.63	-3.09×10^{2}	-6.00×10^{-2}	-8.85×10^{-2}	4.28	116	71.36
								Touchdown	2.26×10^{-2}	4.20×10^{-3}	-1.67	1.94×10^{2}	-1.24×10^{-2}	5.37×10^{-2}	8.86×10^{-1}	123	71.36
18 [c,d]	.0	.0	Medium	None	None	50	30	Start of flare	3.53×10^{-2}	1.28×10^{-2}	-1.55×10^{1}	-2.64×10^{2}	-7.07×10^{-2}	-1.22×10^{-1}	5.40	104	76.49
								Touchdown	2.12×10^{-2}	2.54×10^{-2}	-9.26	3.06×10^{1}	-1.32×10^{-2}	3.43×10^{-2}	1.00	108	75.69
19 [c,d]	.0	.0	Medium	None	None	10	30	Start of flare	3.08×10^{-2}	1.21×10^{-2}	-1.38×10^{1}	-3.19×10^{2}	-7.35×10^{-2}	-1.12×10^{-1}	5.45	104	74.27
								Touchdown	7.24×10^{-3}	9.80×10^{-3}	-8.04	-1.57×10^{1}	-2.84×10^{-2}	9.86×10^{-3}	2.09	108	73.58
20 [c,d]	.0	.0	Medium	None	None	5	30	Start of flare	5.81×10^{-3}	-7.94×10^{-3}	-1.46	-2.74×10^{2}	-7.27×10^{-2}	-1.29×10^{-1}	5.36	116	73.76
								Touchdown	-1.19×10^{-2}	6.54×10^{-3}	-5.61	3.67	-3.19×10^{-2}	3.92×10^{-2}	2.30	119	73.91
21 [c,d,e]	-25.80	$\pi/4$	Patchy	None	None	10	30	Start of flare	-1.53×10^{-2}	1.98×10^{-1}	7.69×10^{-1}	-2.82×10^{2}	-7.13×10^{-2}	-1.74×10^{-1}	5.19	111	72.92
								Touchdown	-1.24×10^{-4}	1.86×10^{-1}	1.21	2.13×10^{2}	-2.37×10^{-2}	-4.63×10^{-2}	1.71	115	72.15
22 [c,d,e]	-25.80	$\pi/4$	Medium	None	None	5	5	Start of flare	5.10×10^{-2}	1.98×10^{-1}	-2.16×10^{1}	-2.76×10^{2}	-4.12×10^{-2}	-1.44×10^{-2}	3.28	99	79.59
								Touchdown	4.26×10^{-3}	2.19×10^{-1}	-9.85	1.36×10^{2}	-1.56×10^{-2}	-2.77×10^{-2}	1.22	104	78.38

[a] V_i = 77.12 for cases 1, 2, 3, 4, 5, 6, 17, 20, and 21; V_i = 78.56 for cases 13 and 14; V_i = 81.32 for case 8; V_i = 91.92 for case 11; V_i = 97.09 for cases 7, 9, 12, 15, 16, 18, 19, and 22; V_i = 102.92 for case 10.

[b] Basic system from NASA TN D-7611 (ref. 1).

[c] This run has β feed to roll-control system and velocity compensation by equation (1), φ_c given by equation (2).

[d] This run has special flap control for pitch angle.

[e] The heading angle of the airplane in this run represents the crab angle with respect to the runway centerline. The velocity vector is pointing down the runway.

[f] Wind shear 0.0478 meter per second per meter.

[g] Wind changed direction from $\pi/4$ at 540 m to $-\pi/4$ at touchdown.

TABLE III.- THE EFFECT OF THE GAIN k_1 ON THE GROUND TRACK AND TOUCHDOWN CONDITIONS

[Initial condition: $\zeta_1 = -3000$ m; $\zeta_2 = 4000$ m; $H = 540$ m; $\psi_i = 0.0$]

	Case 23		Case 24		Case 25		Case 26	
k_1 at A*	2.00		1.796		1.759		1.706	
k_1 at B*	1.98		1.753		1.714		1.665	
T at B, sec	28.6		31.4		31.7		32.0	
φ at B, rad	1.039×10^{-3}		1.27×10^{-3}		9.60×10^{-4}		-8.87×10^{-4}	
ψ at B, rad	1.29		1.38		1.39		1.42	
ζ_1 at B, m	-1813.6		-1825.1		-1834.4		-1851.0	
ζ_2 at B, m	-2548.6		-2327.5		-2253.4		-2252.2	
	Start of flare	Touchdown	Start of flare	Touchdown	Start of flare	Touchdown	Start of flare	Touchdown
φ, rad	-1.75×10^{-1}	-2.65×10^{-1}	-2.18×10^{-1}	-1.12×10^{-1}	-1.78×10^{-1}	-1.95×10^{-2}	-1.24×10^{-1}	-3.35×10^{-3}
ψ, rad	4.15×10^{-1}	2.0×10^{-1}	2.97×10^{-1}	2.08×10^{-7}	2.61×10^{-1}	2.10×10^{-1}	2.21×10^{-1}	1.90×10^{-1}
ζ_2, m	-1.14×10^{2}	-67.8	-41.81	-9.09	-29.9	-4.24	13.29	4.83×10^{-2}
ζ_1, m	-2.48×10^{2}	-73.3	-334.1	-40.9	-334.4	158.8	-331.1	807.9
γ, rad	-1.43×10^{-1}	-6.86×10^{-2}	-9.82×10^{-2}	-2.61×10^{-2}	-7.43×10^{-2}	-4.83×10^{-3}	-5.32×10^{-2}	-5.30×10^{-3}
θ, rad	-2.46×10^{-1}	-7.62×10^{-2}	-1.78×10^{-1}	-6.88×10^{-2}	-1.41×10^{-1}	2.07×10^{-2}	-1.18×10^{-1}	9.95×10^{-2}
w_{z_j}, m/sec	10.45	4.91	7.85	2.069	5.41	3.38×10^{-1}	3.83	3.86×10^{-1}
Time, sec	71.0	73.5	73	76.6	74	80.9	75	90.8
V, m/sec	73.4	71.6	80.1	79.3	72.9	70.0	72.0	72.8

*See figure 11 for definition of these points.

TABLE IV.- THE EFFECT OF VARYING THE GAIN k_2 ON TOUCHDOWN CONDITIONS, $k_2 = \frac{k_4}{k_1} e^{-|\psi_c - \psi|}$

[Initial condition: ζ_1 = 3000 m; ζ_2 = -4000 m; H = 540 m; ψ = 0.0; k_1 as in cases 23 and 25 of table III]

	Case 23		Case 23a		Case 23b		Case 23c		Case 25		Case 25a		Case 25b	
k_4	4.8		3.8		3.2		3.0		4.8		4.4		4.0	
	Start of flare	Touchdown	Start of flare	Touchdown	Start of flare	Touchdown	Start of flare	Touchdown	Start of flare	Touchdown	Start of flare	Touchdown	Start of flare	Touchdown
φ, rad	-1.75×10^{-1}	-2.65×10^{-1}	-2.28×10^{-1}	-2.78×10^{-1}	-2.70×10^{-1}	-3.11×10^{-1}	-2.88×10^{-1}	-2.79×10^{-1}	-1.78×10^{-1}	-1.95×10^{-2}	-1.89×10^{-1}	2.48×10^{-3}	-2.20×10^{-1}	3.32×10^{-2}
ψ, rad	4.15×10^{-1}	2.0×10^{-1}	3.53×10^{-1}	2.57×10^{-1}	3.42×10^{-1}	2.29×10^{-1}	3.42×10^{-1}	2.11×10^{-1}	2.61×10^{-1}	2.10×10^{-1}	2.37×10^{-1}	1.96×10^{-1}	2.19×10^{-1}	1.69×10^{-1}
ζ_2, m	-1.14×10^{2}	-67.8	-58.6	-34.2	-13.16	-9.77	47.8	29.1	-29.9	-4.24	-10.35	1.94×10^{-1}	13.0	4.1
ζ_1, m	-2.48×10^{2}	-73.3	-243.5	-128.2	-294.2	-170.4	-321.5	-171.9	-334.4	158.8	-337.9	196.4	-349.5	258.7
γ, rad	-1.43×10^{-1}	-6.86×10^{-2}	-1.42×10^{-1}	-7.32×10^{-2}	-1.43×10^{-1}	-8.22×10^{-2}	-1.42×10^{-1}	-7.07×10^{-2}	-7.43×10^{-2}	-4.83×10^{-3}	-7.24×10^{-2}	-7.47×10^{-3}	-7.12×10^{-2}	-1.0×10^{-2}
θ, rad	-2.46×10^{-1}	-7.62×10^{-2}	-1.88×10^{-1}	-9.03×10^{-2}	-2.19×10^{-1}	-9.97×10^{-2}	-2.21×10^{-1}	-9.42×10^{-2}	-1.41×10^{-1}	2.07×10^{-2}	-1.40×10^{-1}	3.02×10^{-2}	-1.48×10^{-1}	3.76×10^{-2}
w_{z_j}, m/sec	10.45	4.91	10.49	5.43	10.63	6.13	10.39	5.06	5.41	3.38×10^{-1}	5.29	5.21×10^{-1}	5.36	7.17×10^{-1}
Time, sec	71.0	73.5	72.0	73.6	72.0	73.6	72.0	74.1	74.0	80.9	74.0	81.6	74.0	82.3
V, m/sec	73.4	71.6	74.1	74.3	74.6	74.7	73.4	71.6	72.9	70.0	73.1	69.7	75.3	71.7

TABLE V.- SUMMARY OF RESULTS OBTAINED USING NEW METHODS TO DETERMINE k_1 AND k_2

[Windspeed = -25.80 m/sec at $\pi/4$ rad; patchy turbulence; sample rate 10 per second]

	Case 27a		Case 27b		Case 27c		Case 28a		Case 28b		Case 28c	
ζ_1, m	-6000		-6000		-6000		-3000		-3000		-3000	
ζ_2, m	-4000		-4000		-4000		-4000		-4000		-4000	
H, m	540		540		540		540		540		540	
ψ_i, rad	.0		$\pi/4$		$\pi/2$		.0		$\pi/4$		$\pi/2$	
	Start of flare	Touchdown	Start of flare	Touchdown	Start of flare	Touchdown	Start of flare	Touchdown	Start of flare	Touchdown	Start of flare	Touchdown
φ, rad	-5.64×10^{-3}	2.36×10^{-2}	-1.10×10^{-2}	2.49×10^{-2}	3.04×10^{-3}	-3.66×10^{-3}	-1.51×10^{-1}	1.52×10^{-2}	-7.89×10^{-2}	1.91×10^{-2}	-8.00×10^{-2}	-1.04×10^{-2}
ψ, rad	1.95×10^{-1}	1.86×10^{-1}	1.95×10^{-1}	1.97×10^{-1}	1.94×10^{-1}	1.85×10^{-1}	2.03×10^{-1}	1.87×10^{-1}	2.04×10^{-1}	1.99×10^{-1}	2.32×10^{-1}	1.84×10^{-1}
ζ_2, m	4.25×10^{-1}	4.18×10^{-1}	1.23	-1.27×10^{-1}	-6.46×10^{-2}	6.82×10^{-1}	1.51	3.66×10^{-1}	-4.93×10^{-1}	-2.88×10^{-1}	1.57×10^{1}	-1.05
ζ_1, m	-2.91×10^{2}	2.32×10^{2}	-2.88×10^{2}	1.37×10^{2}	-2.96×10^{2}	8.45	-3.02×10^{2}	3.44×10^{2}	-3.36×10^{2}	5.18×10^{1}	-3.51×10^{2}	8.72×10^{2}
γ, rad	-4.12×10^{-2}	-9.93×10^{-3}	-5.65×10^{-2}	-1.63×10^{-2}	-6.23×10^{-2}	-7.79×10^{-3}	-4.74×10^{-2}	-1.15×10^{-2}	-7.70×10^{-2}	-1.41×10^{-2}	-6.31×10^{-2}	-2.61×10^{-3}
θ, rad	-1.58×10^{-1}	1.60×10^{-2}	-1.70×10^{-1}	-9.56×10^{-3}	-1.70×10^{-1}	-3.33×10^{-2}	-1.19×10^{-1}	5.68×10^{-2}	-1.40×10^{-1}	5.86×10^{-3}	-1.38×10^{-1}	1.04×10^{-1}
w_{z_j}, m/sec	2.98	7.27×10^{-1}	4.06	1.18	4.50	5.68×10^{-1}	3.54	8.34×10^{-1}	5.61	9.83×10^{-1}	4.78	1.95×10^{-1}
Time, sec	114.0	121.7	117.0	122.8	116.0	120.2	75.0	83.8	74.0	79.5	75.0	91.3
V, m/sec	72.28	73.24	71.91	72.45	72.24	72.94	74.69	72.49	72.97	69.65	75.86	74.7

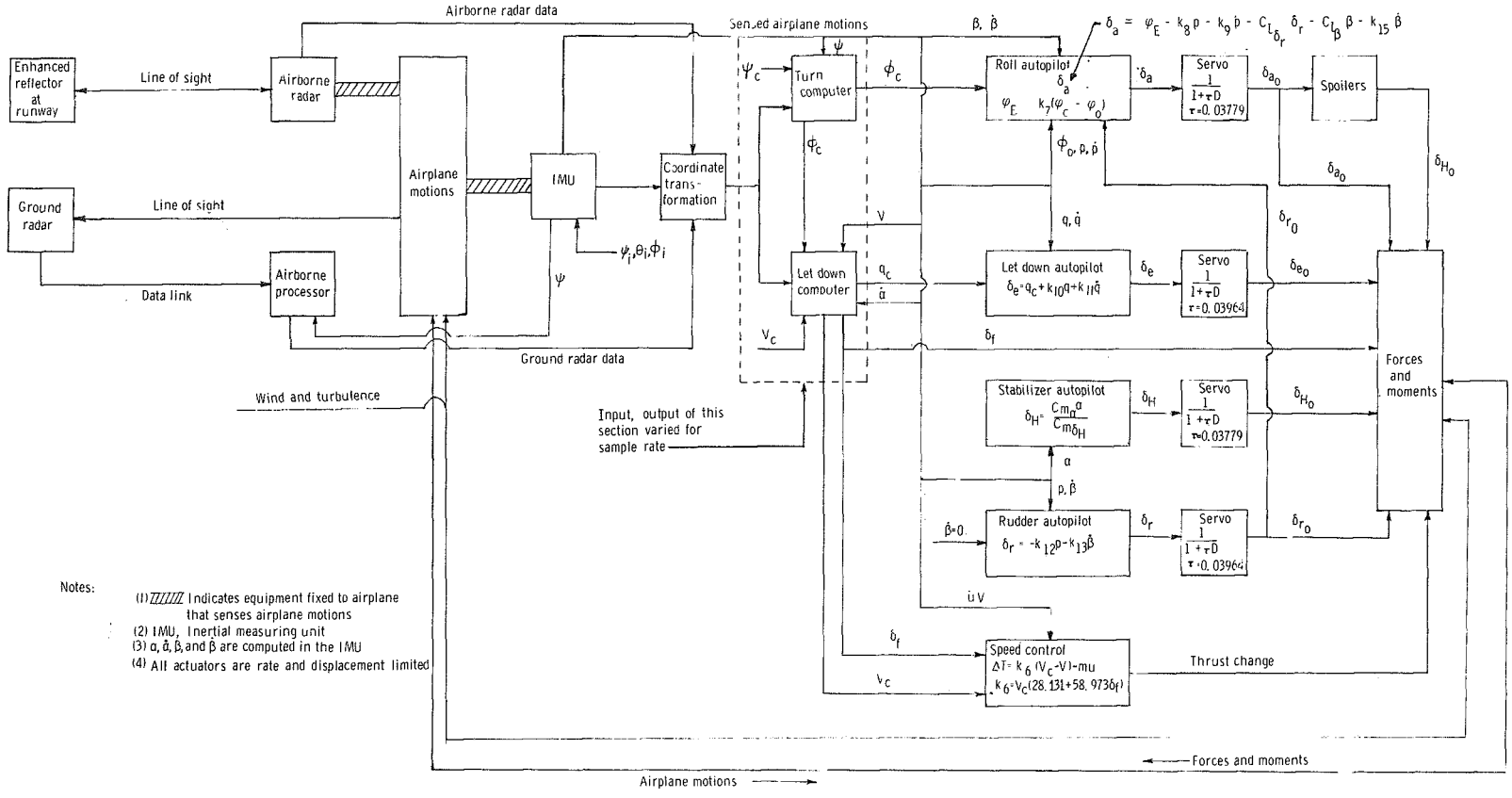

Figure 1.- Block diagram of the automatic landing system. Symbols are defined in reference 1.

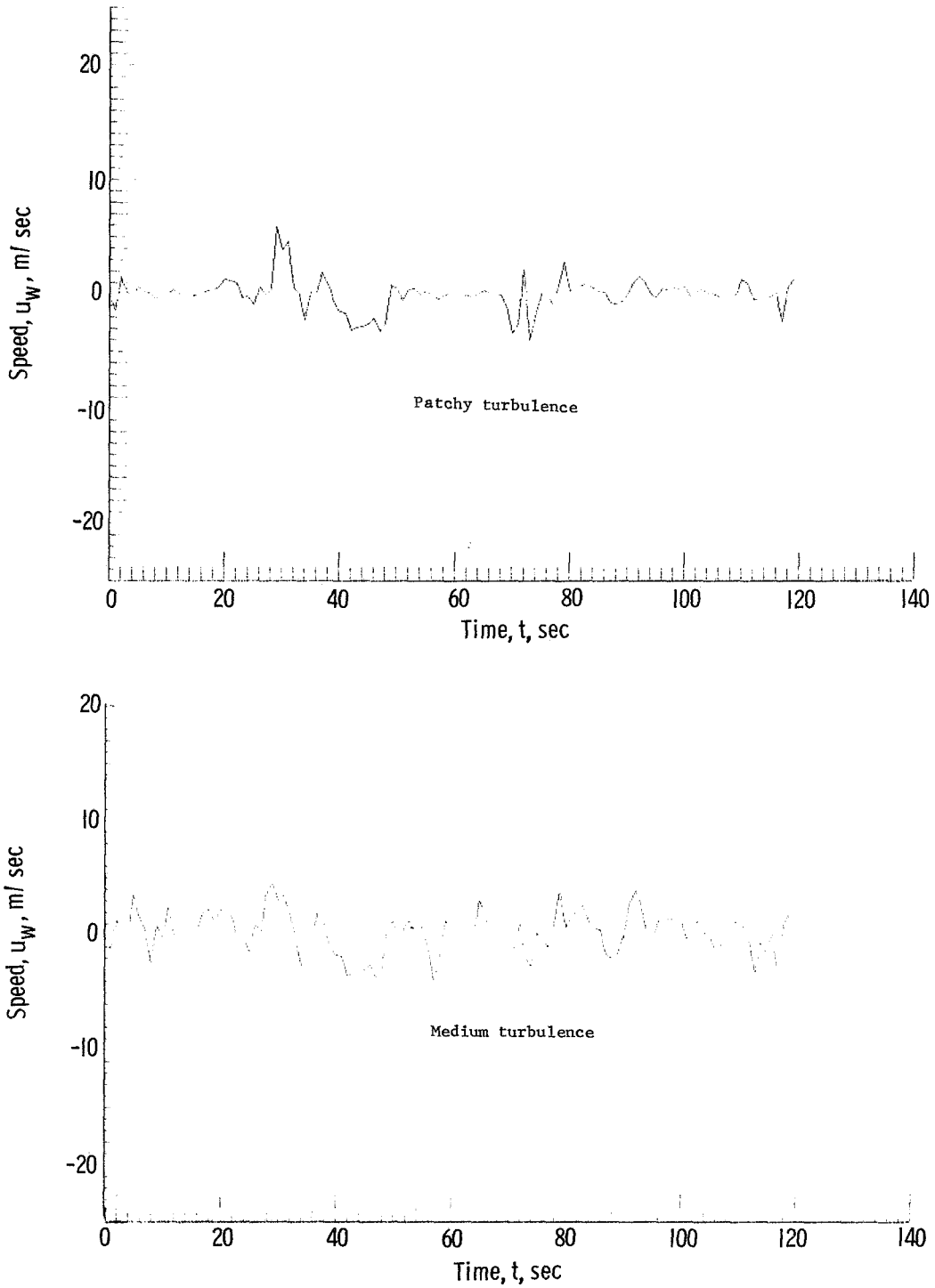

(a) Turbulence along η_1-axis.

Figure 2.- Turbulence used in study.

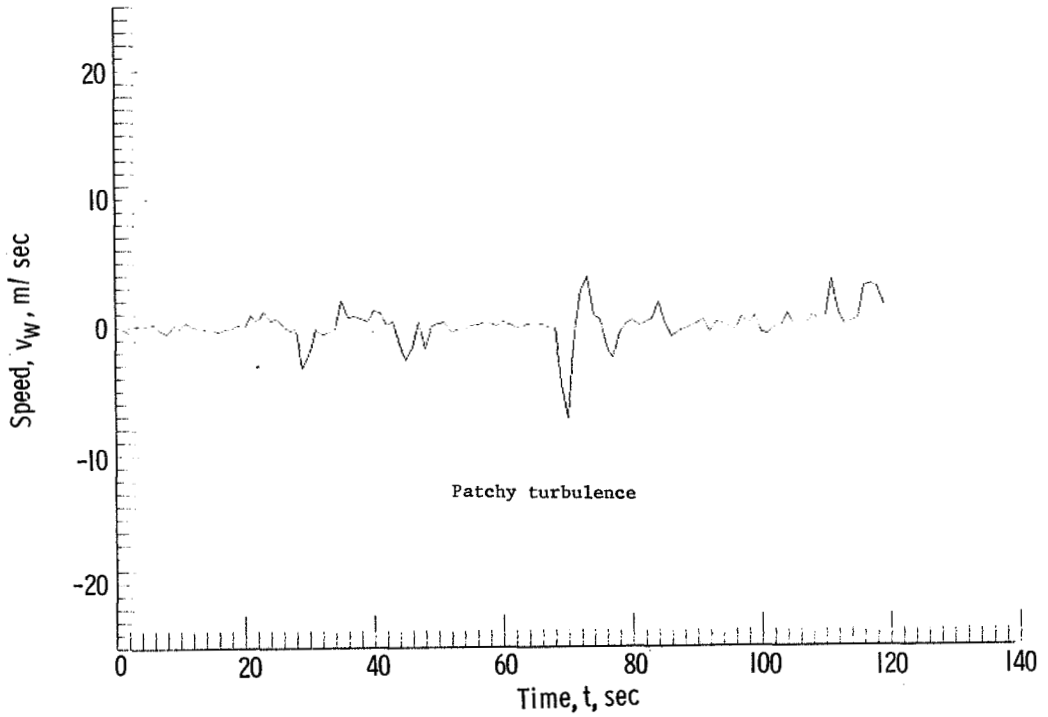

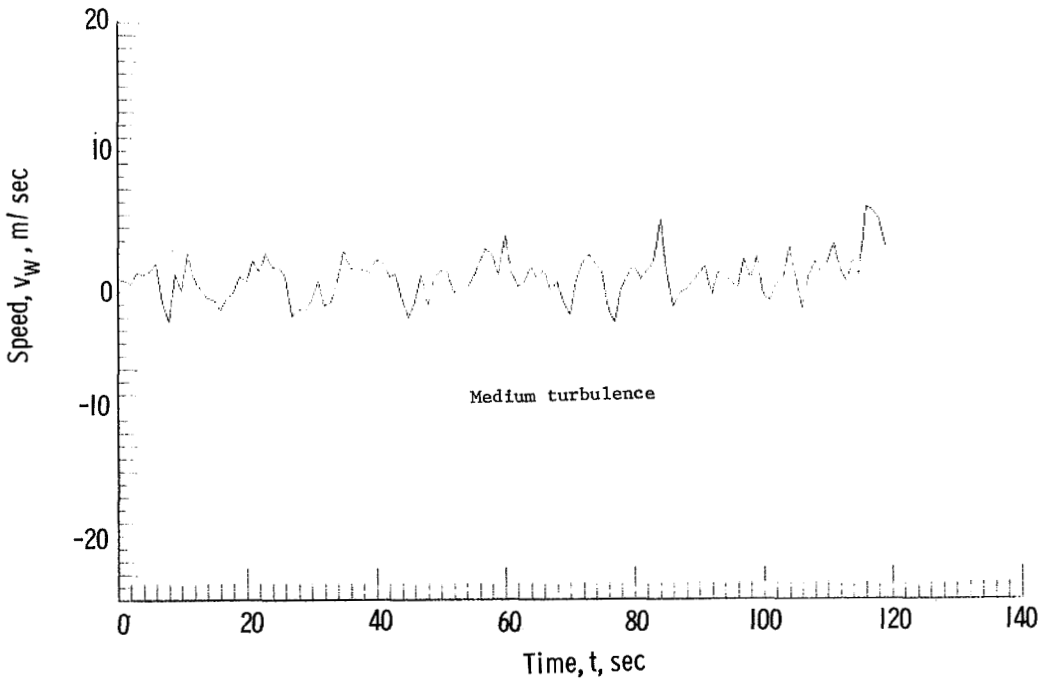

(b) Turbulence along η_2-axis.

Figure 2.- Continued.

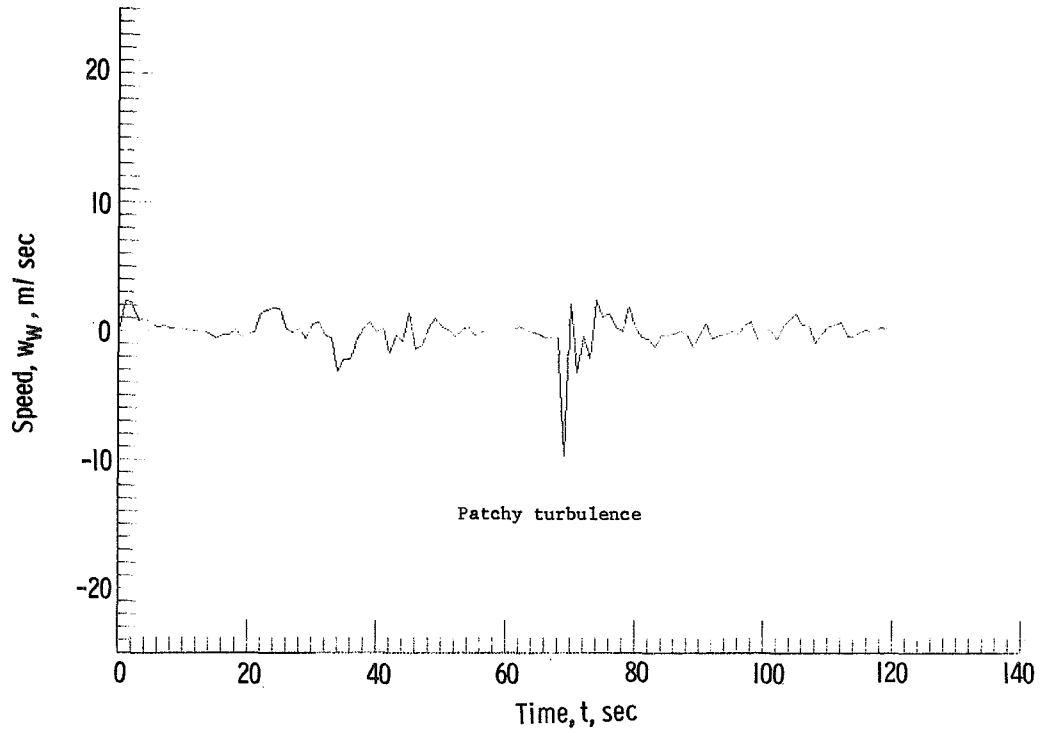

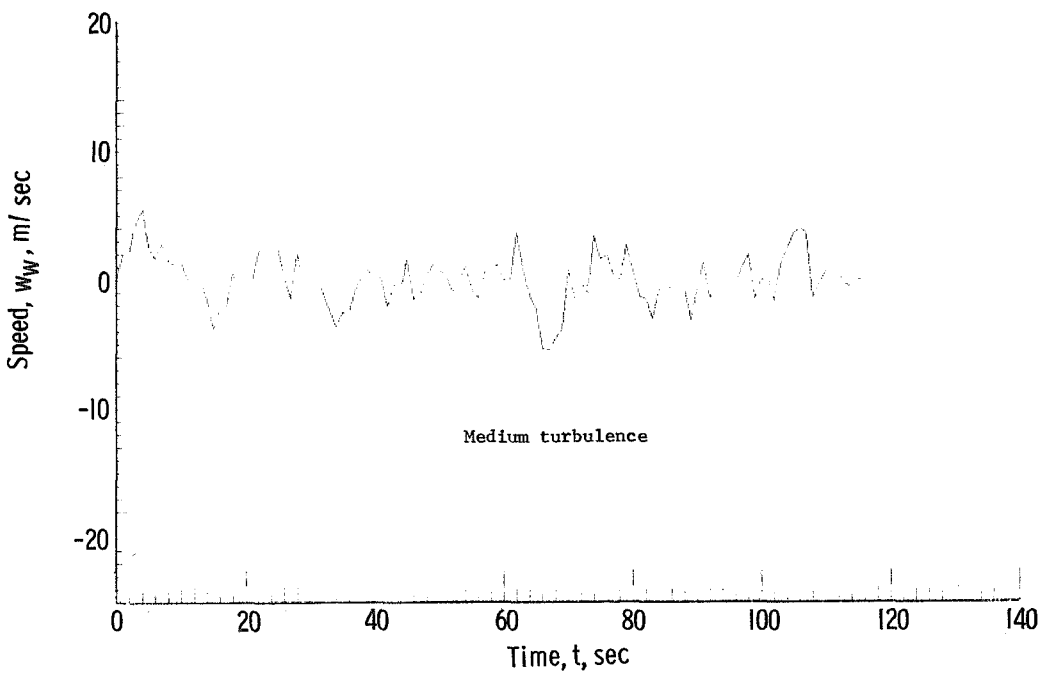

(c) Turbulence along η_3-axis.

Figure 2.- Concluded.

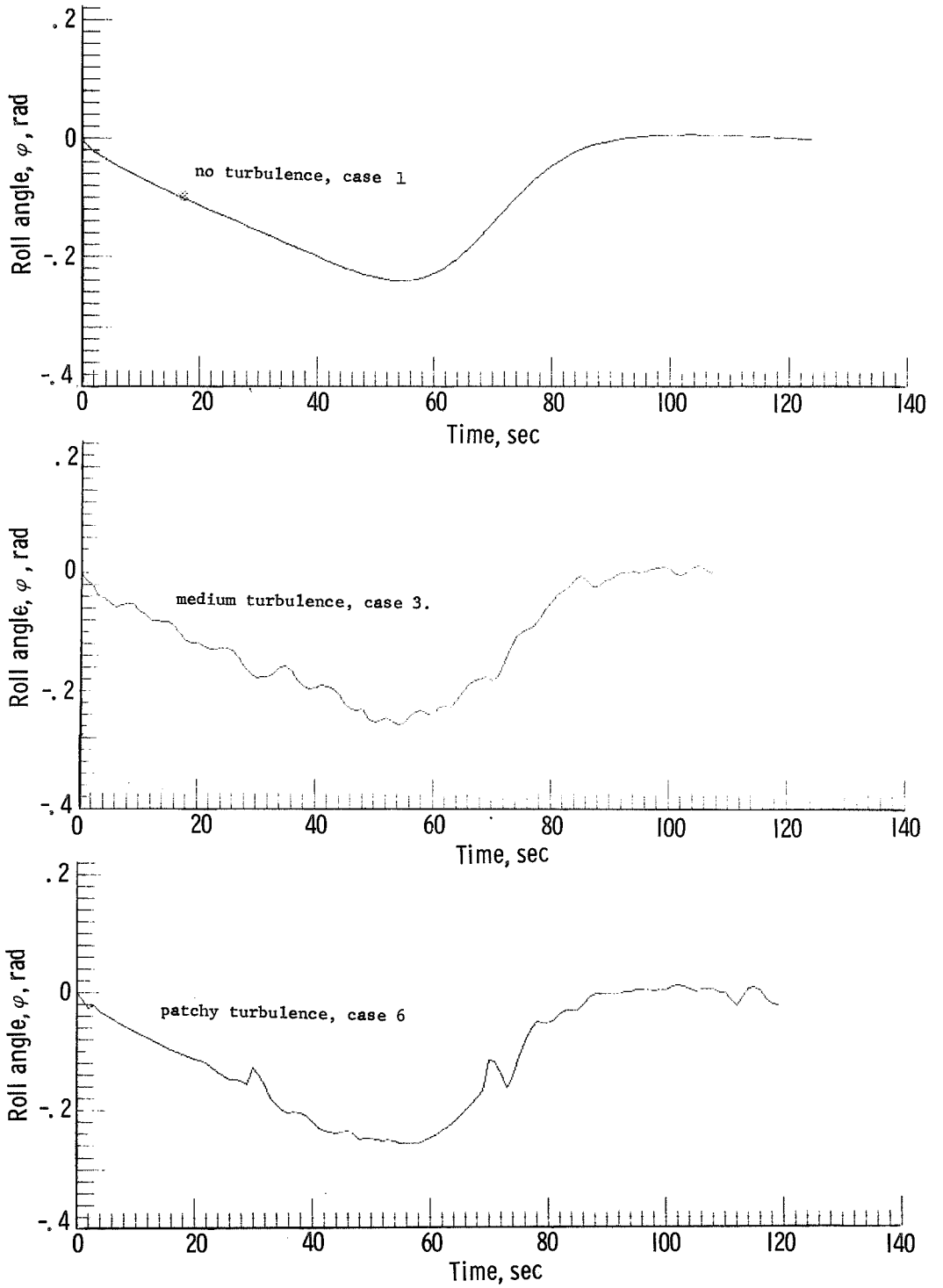

(a) Roll response.

Figure 3.- The effect of turbulence on selected airplane states during a typical landing maneuver. Penetration effects are not included.

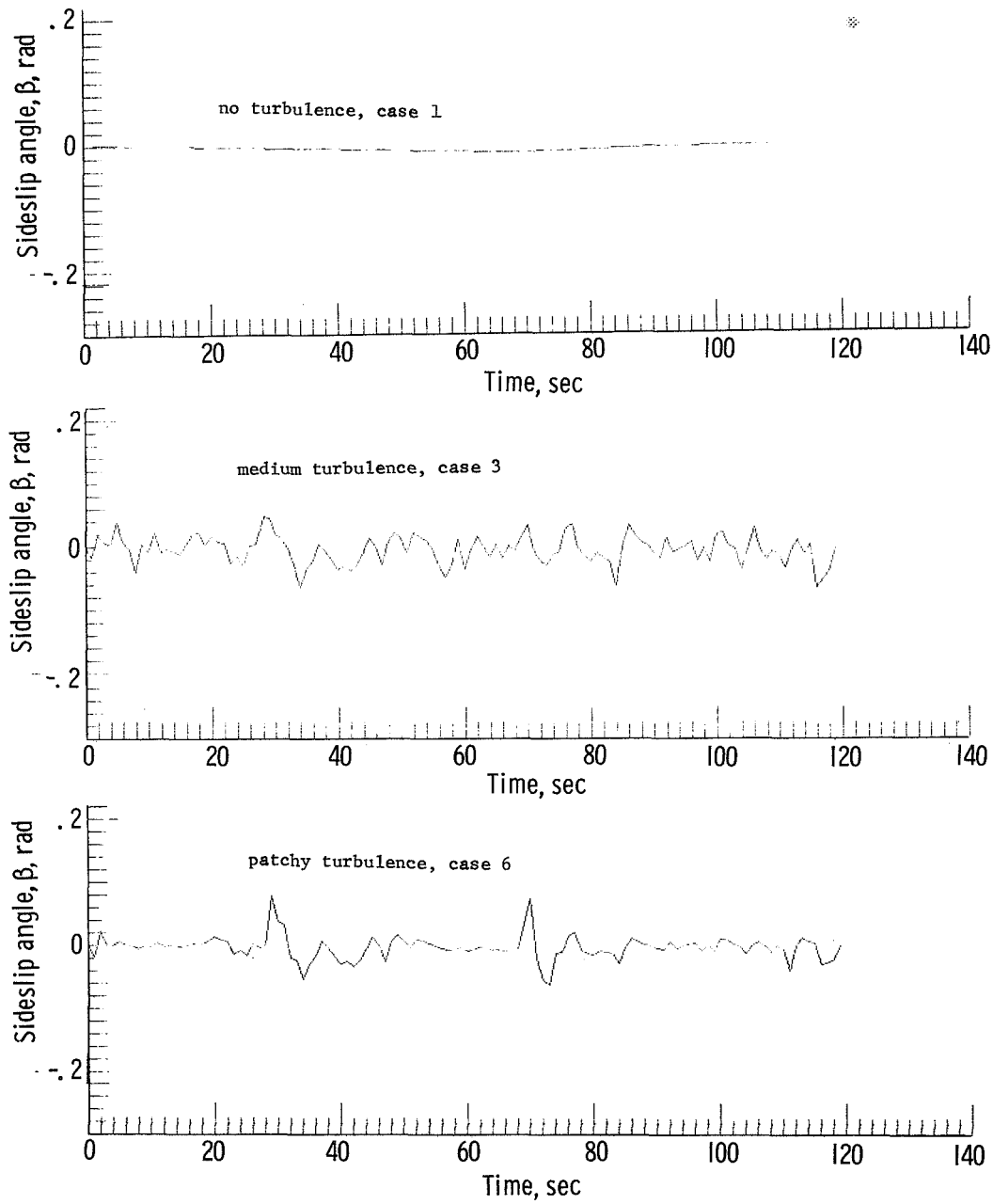

(b) Sideslip angle.

Figure 3.- Continued.

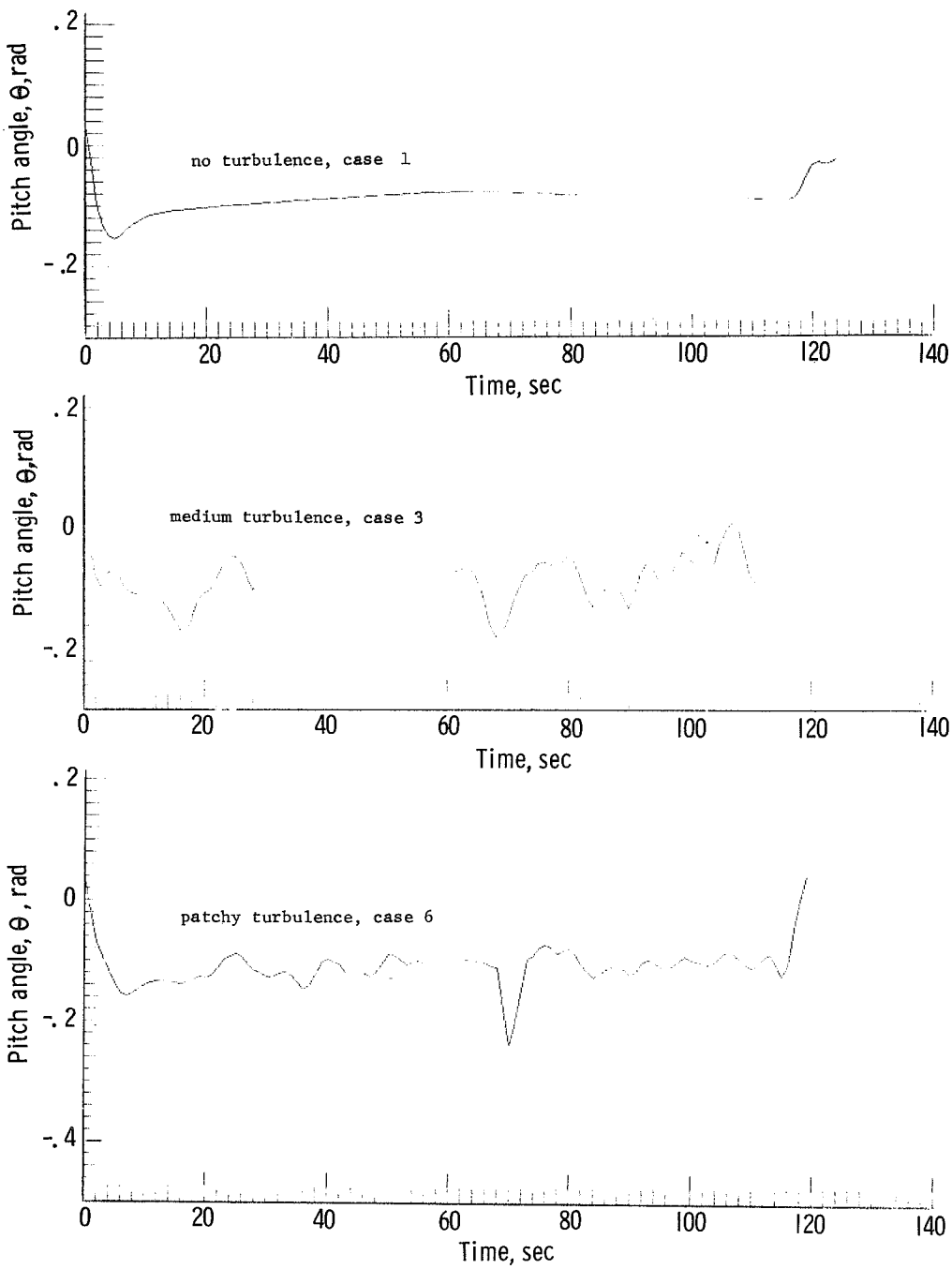

(c) Pitch angle.

Figure 3.- Continued.

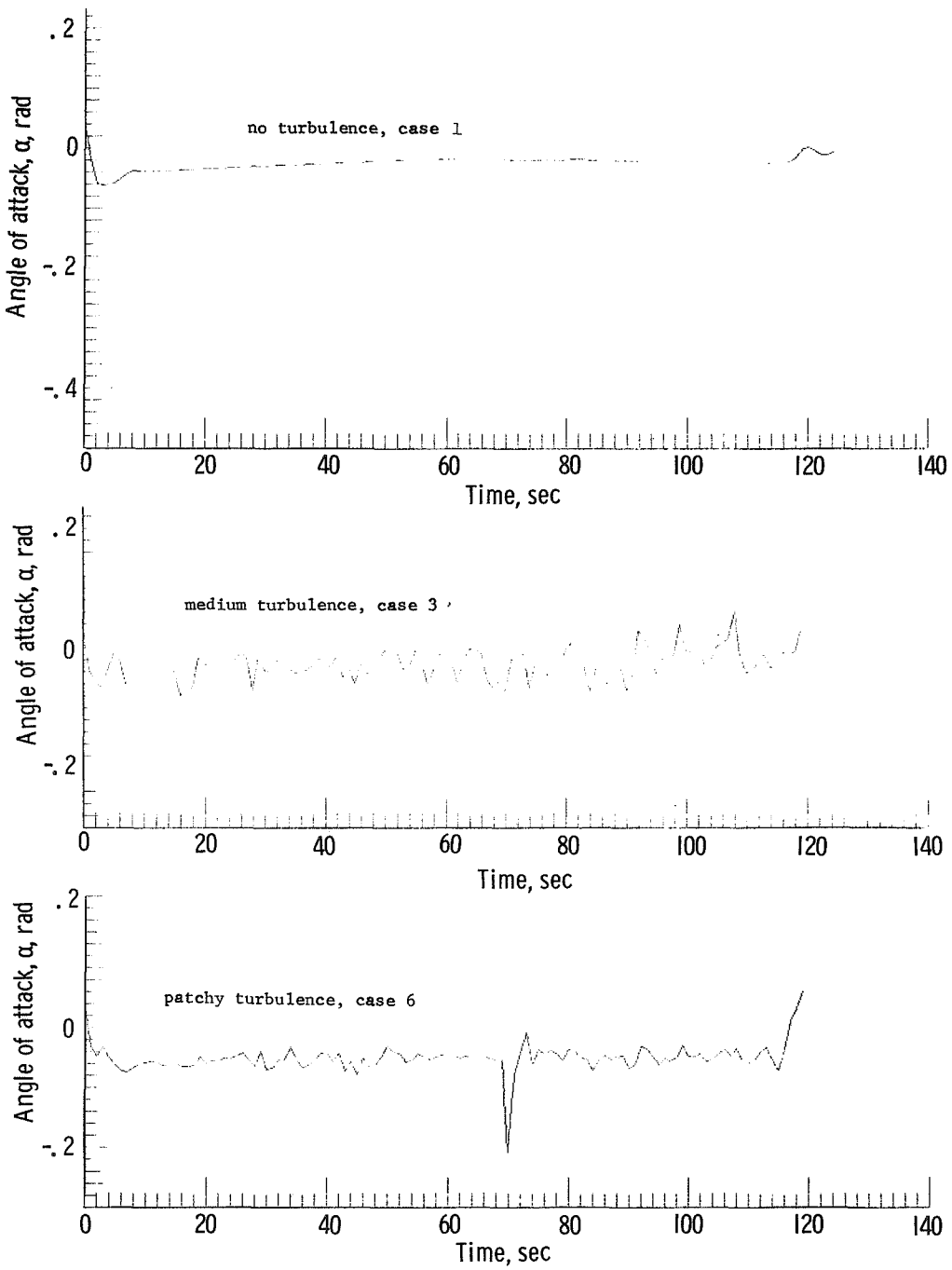

(d) Angle of attack.

Figure 3.- Continued.

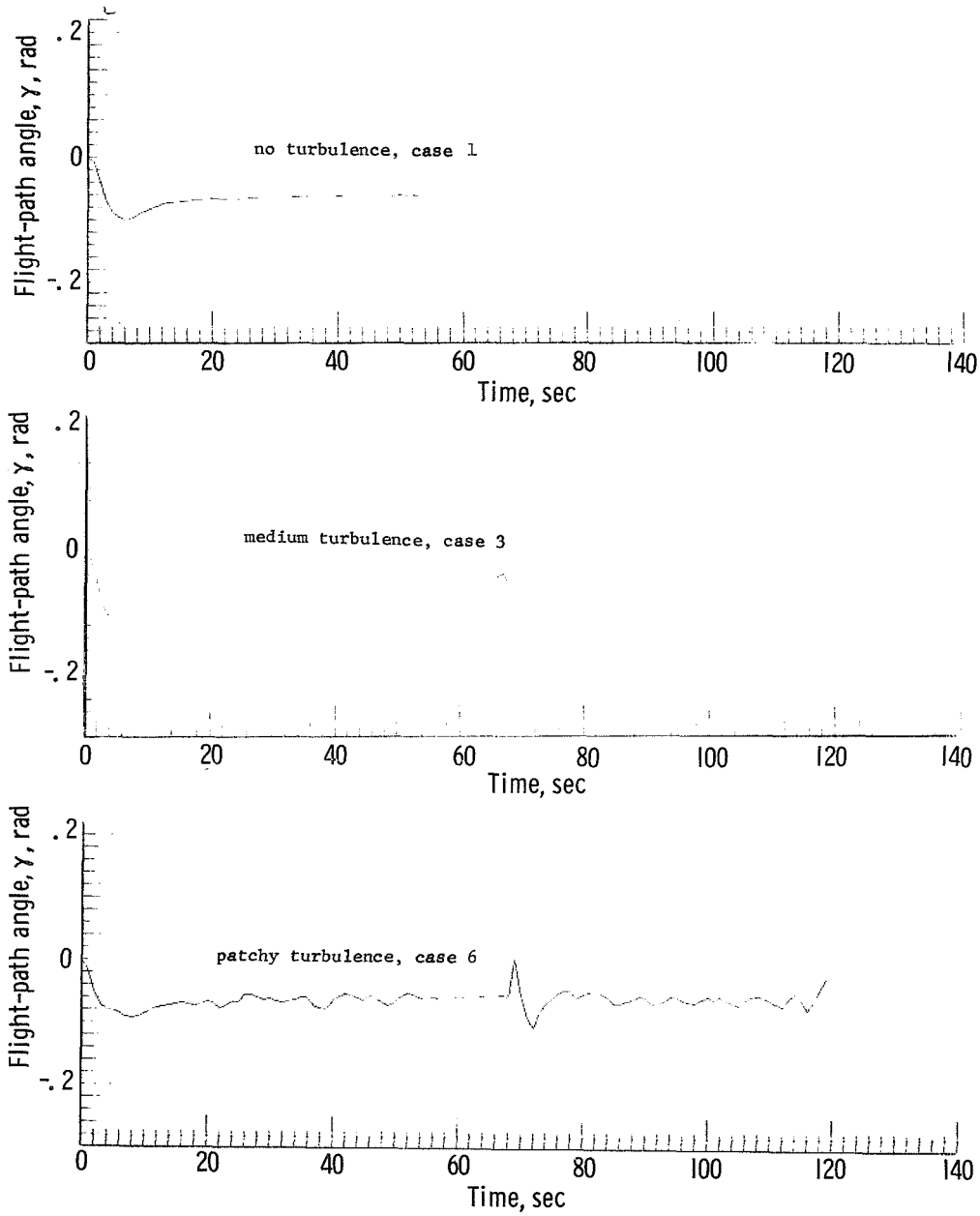

(e) Flight-path angle.

Figure 3.- Concluded.

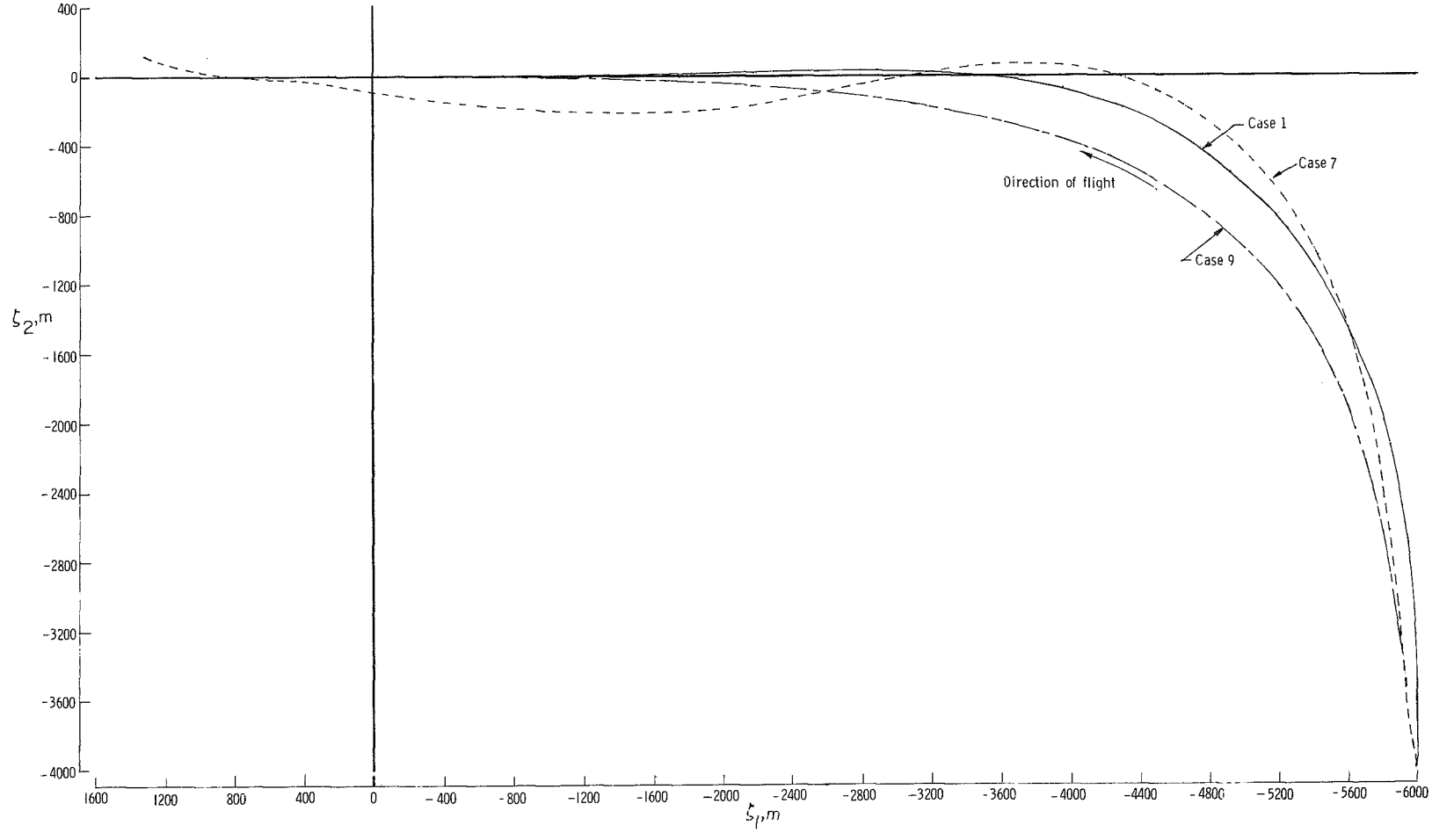

Figure 4.- Effect of steady wind on basic case. Windspeed -25.80 m/sec at angle of $\pi/4$ rad.

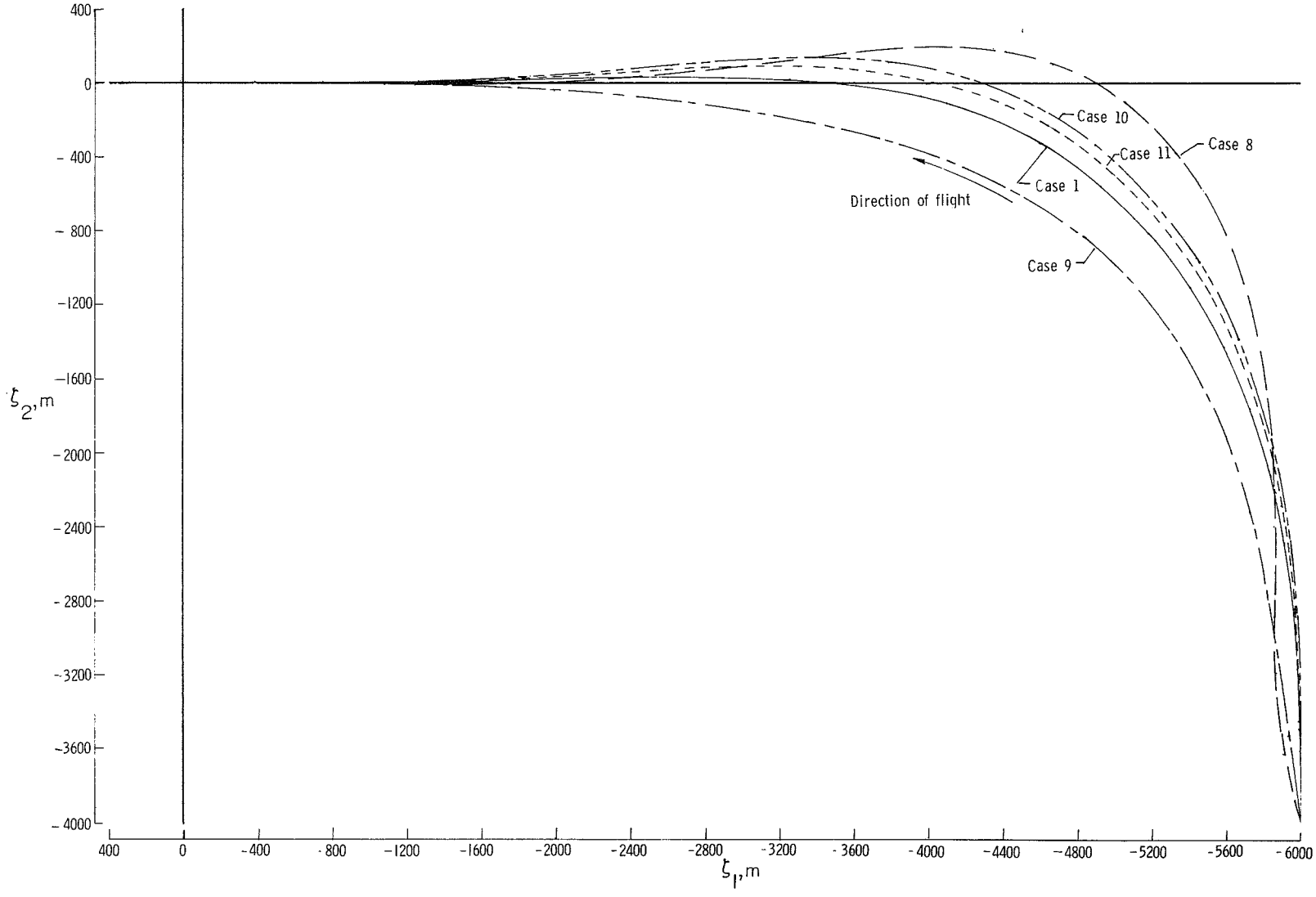

Figure 5.- Effect of steady wind on ground track of velocity compensated basic system.

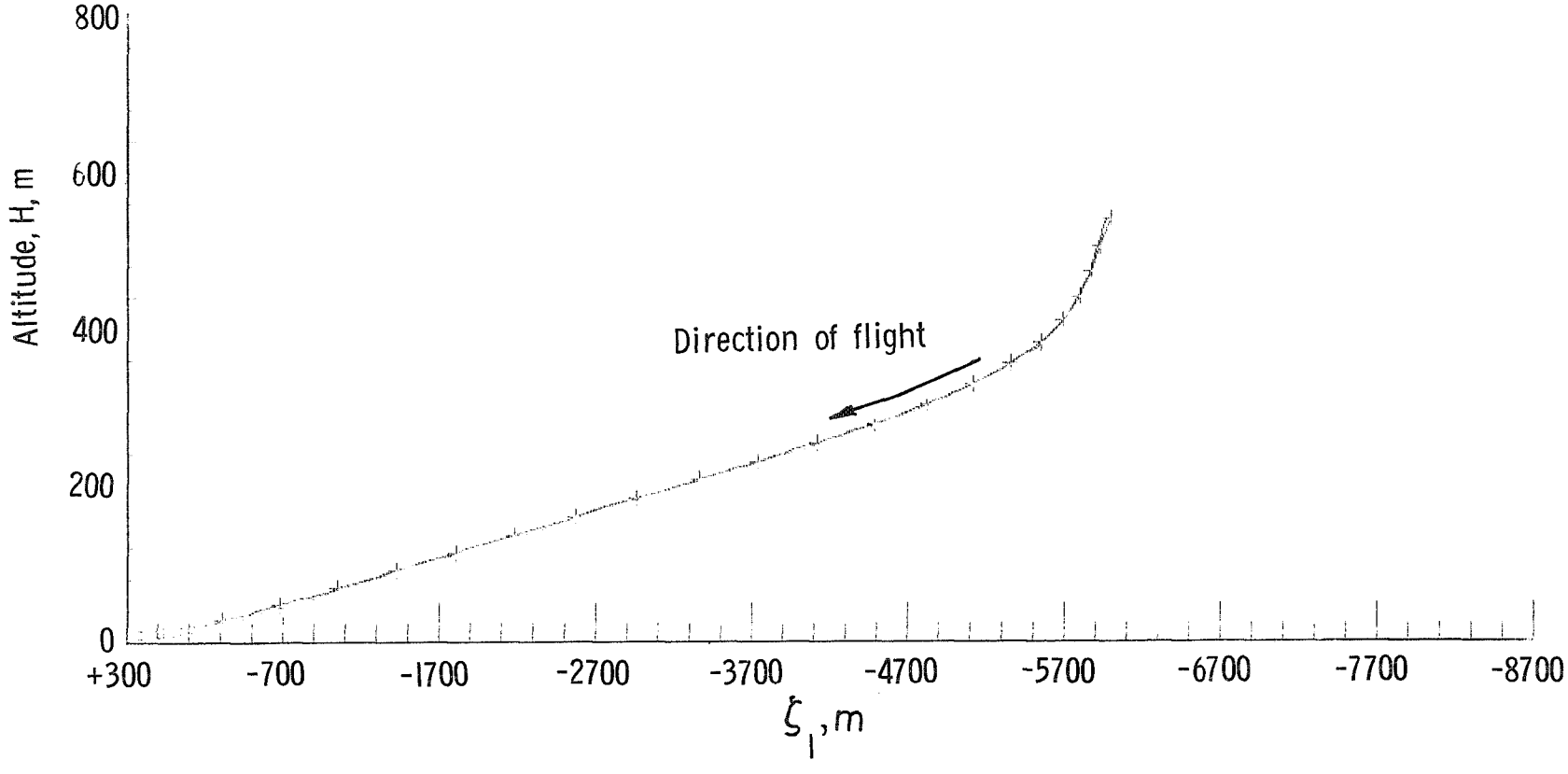

(a) Altitude track.

Figure 6.- Ground and altitude tracks for the initial condition ζ_1 = -6000 m; ζ_2 = -4000 m; H = 540 m; $\psi_i = \pi/2$; windspeed -25.80 m/sec at $\pi/4$; and medium turbulence.

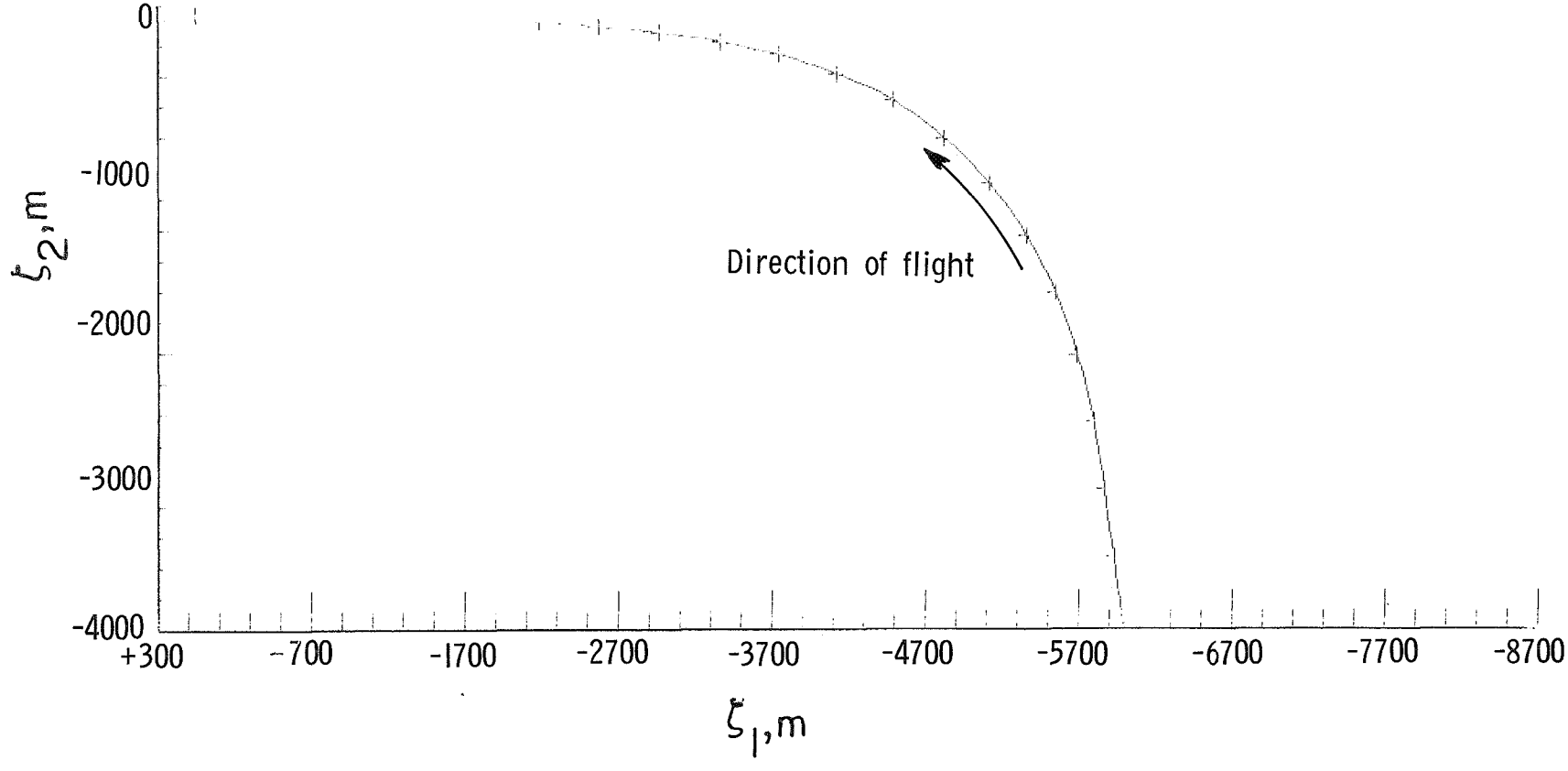

(b) Ground track.

Figure 6.- Concluded.

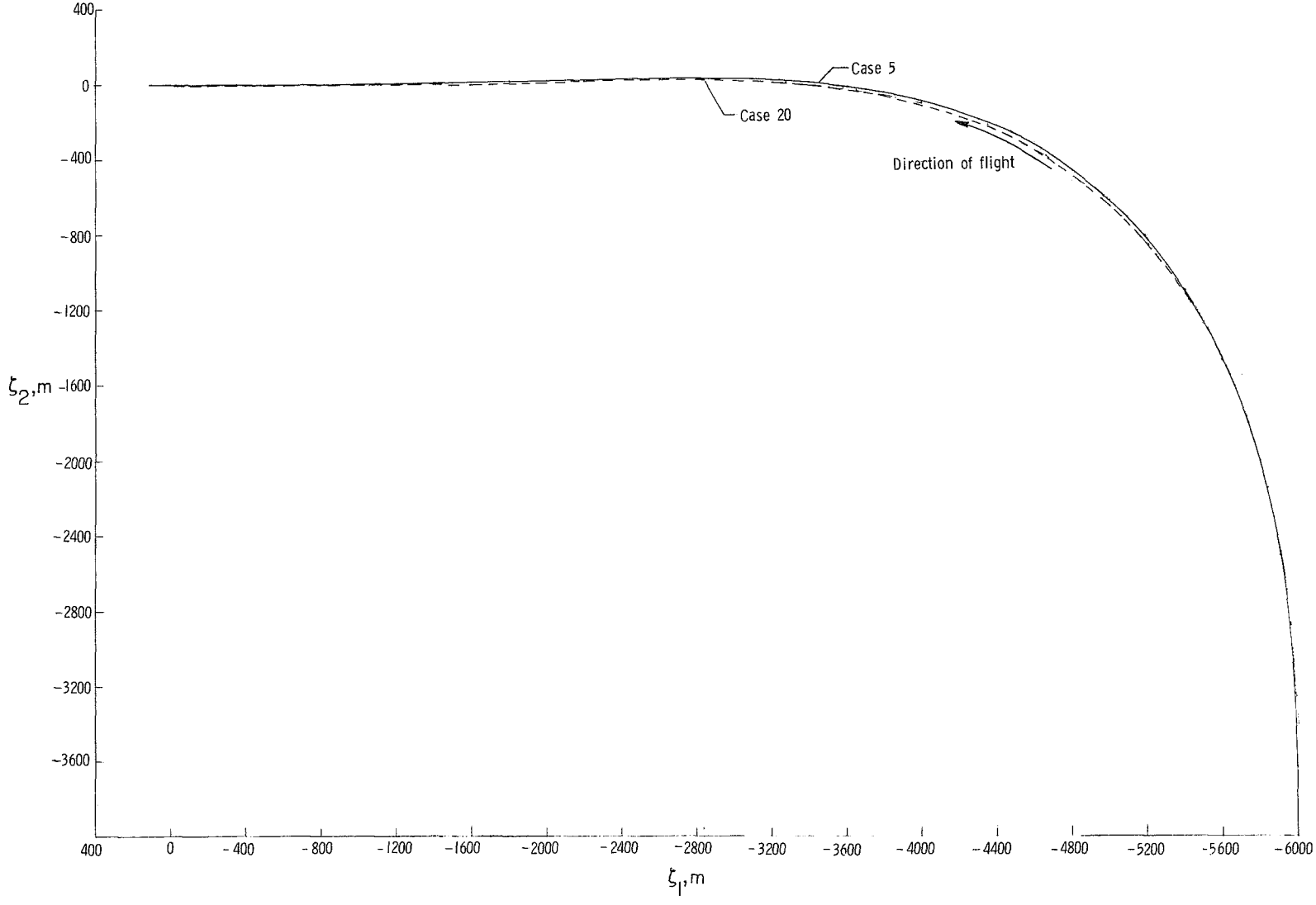

Figure 7.- Effect of sample rate on ground track.

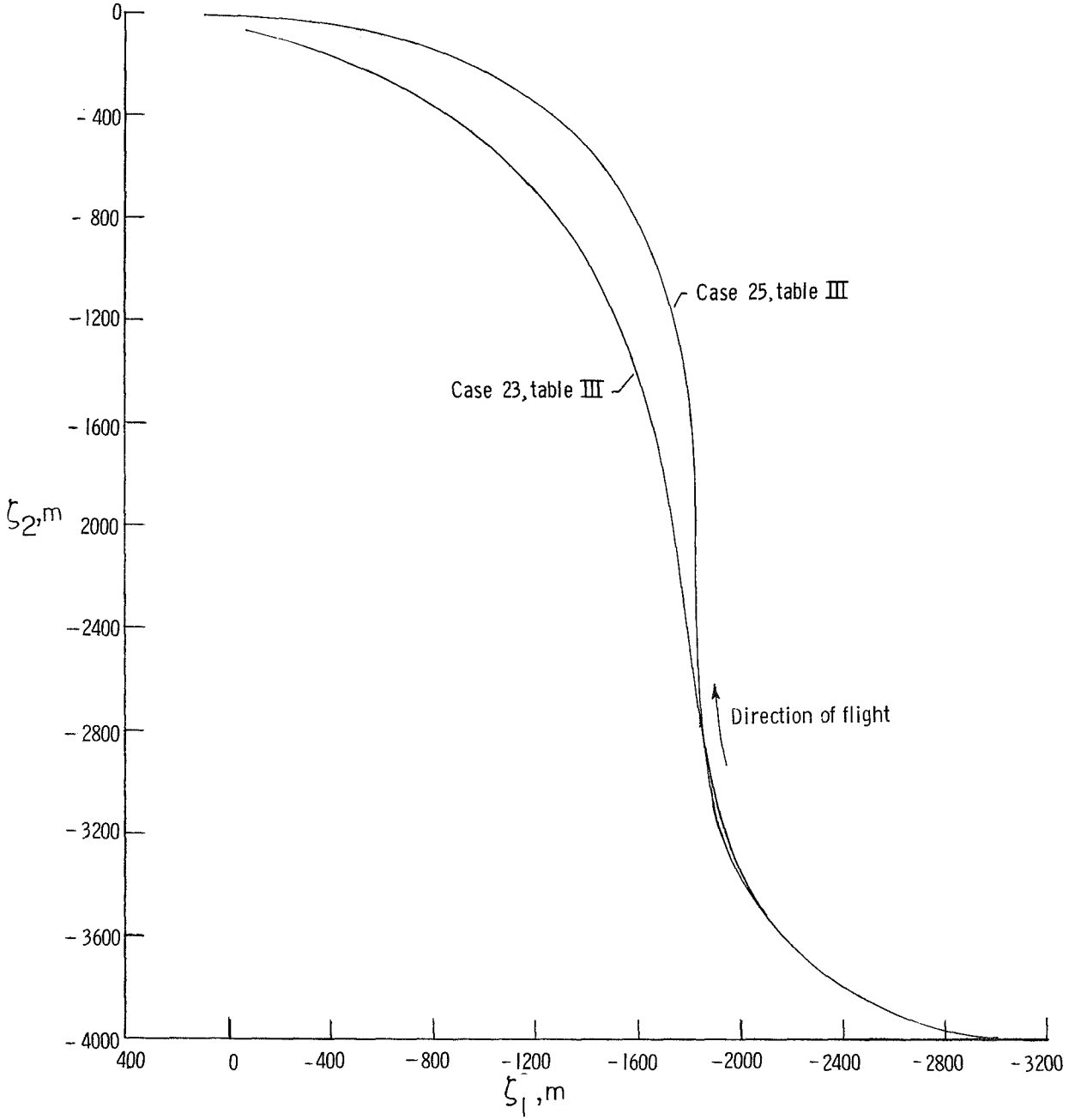

Figure 8.- Comparison of ground tracks for correct, case 25, and incorrect, case 23, settings of k_1.

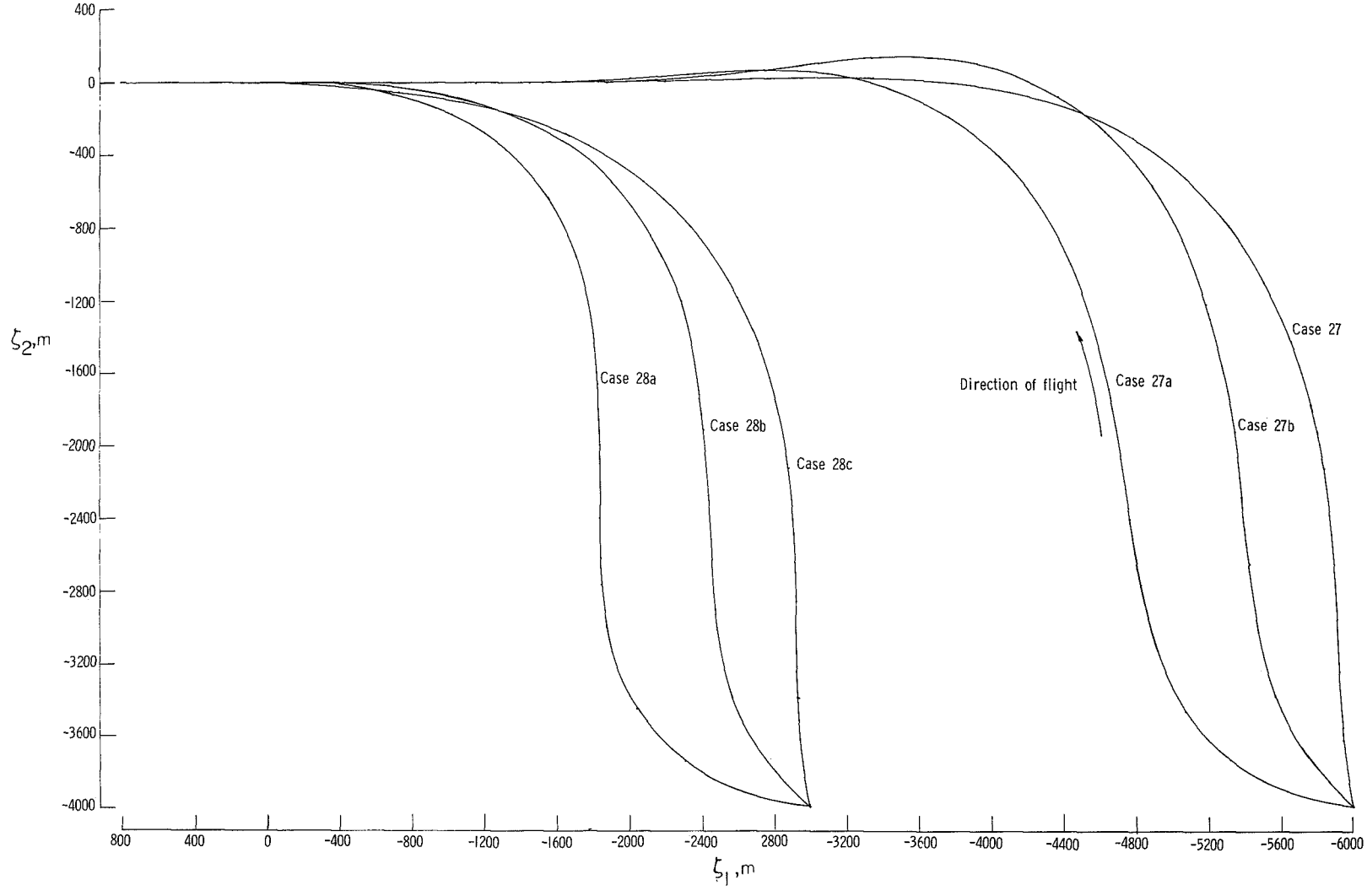

Figure 9.- Comparison of ground tracks for final method of determining k_1 and k_2. Patchy turbulence and wind -25.80 m/sec at $\pi/4$ rad. Details of initial condition and final conditions are given in table V.

Notes

(1) Runway coordinates are centered at touchdown point; positive directions shown at right

(2) Airplane inertial coordinates are // to runway coordinates but centered in airplane

(3) The z_1 coordinates are centered in the airplane and rotated away from the airplane inertial coordinates by the Euler angle ψ, the heading angle of the airplane. The following sketch shows these relationships:

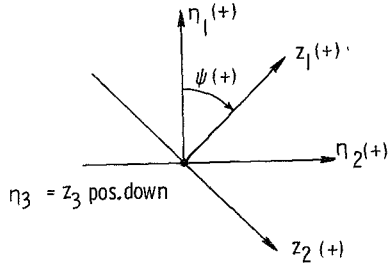

(4) For the runway $\psi = \psi_r = 0$

(5) The η_1, η_2 plane coincides with the z_1, z_2 plane

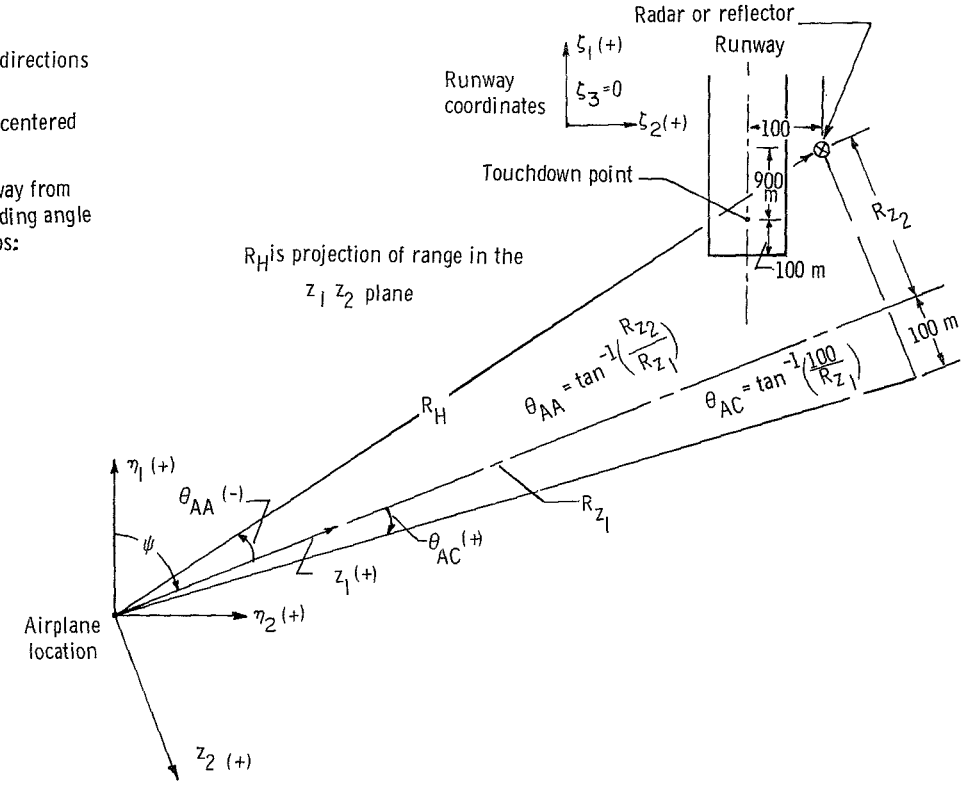

Figure 10.- Geometry of a typical landing situation that shows coordinate systems used in study.

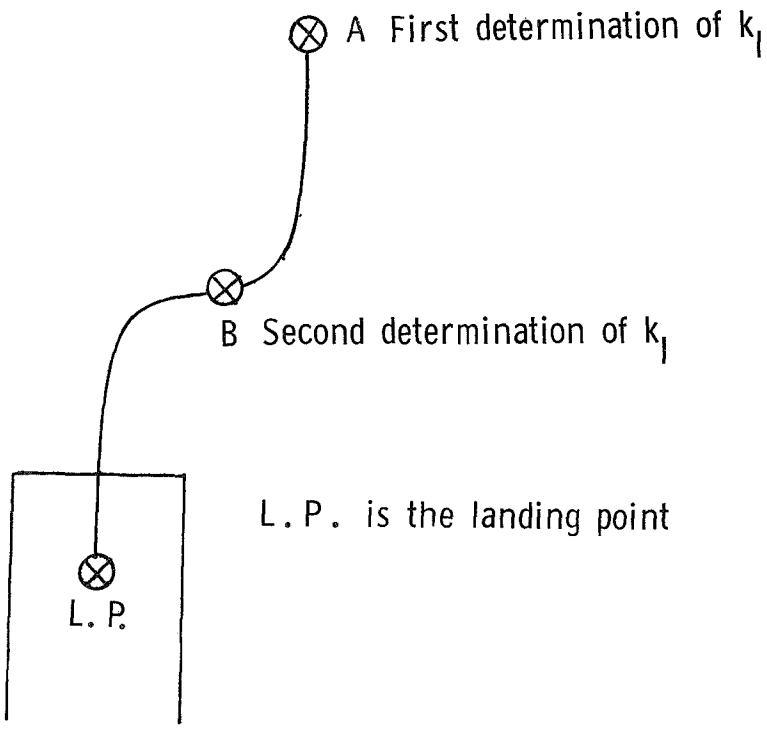

Figure 11.- Sketch of ground track when $\psi_i = 0$.

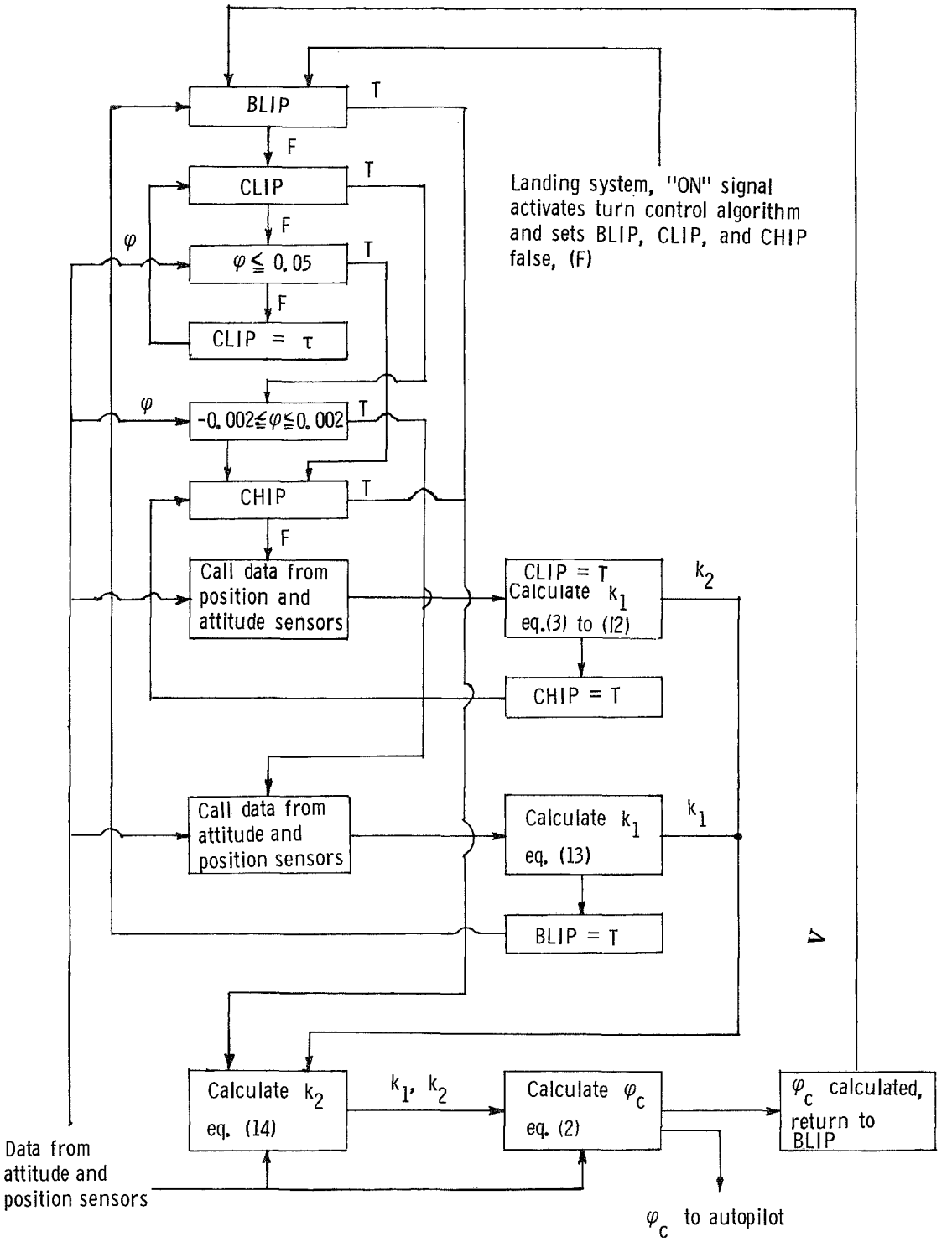

Notes:- (1) This diagram assumes zero roll angle at the start of the landing maneuver

(2) BLIP, CLIP, and CHIP are switch variables and are either true (T) or false (F)

Figure 12.- Turn-control algorithm. Equation numbers refer to equations in the text.

NATIONAL AERONAUTICS AND SPACE ADMINISTRATION
WASHINGTON, D.C. 20546

OFFICIAL BUSINESS
PENALTY FOR PRIVATE USE $300

SPECIAL FOURTH-CLASS RATE BOOK

POSTAGE AND FEES PAID
NATIONAL AERONAUTICS AND SPACE ADMINISTRATION
451

U.S.MAIL

POSTMASTER: If Undeliverable (Section 158 Postal Manual) Do Not Return

"The aeronautical and space activities of the United States shall be conducted so as to contribute . . . to the expansion of human knowledge of phenomena in the atmosphere and space. The Administration shall provide for the widest practicable and appropriate dissemination of information concerning its activities and the results thereof."

—NATIONAL AERONAUTICS AND SPACE ACT OF 1958

NASA SCIENTIFIC AND TECHNICAL PUBLICATIONS

TECHNICAL REPORTS: Scientific and technical information considered important, complete, and a lasting contribution to existing knowledge.

TECHNICAL NOTES: Information less broad in scope but nevertheless of importance as a contribution to existing knowledge.

TECHNICAL MEMORANDUMS: Information receiving limited distribution because of preliminary data, security classification, or other reasons. Also includes conference proceedings with either limited or unlimited distribution.

CONTRACTOR REPORTS: Scientific and technical information generated under a NASA contract or grant and considered an important contribution to existing knowledge.

TECHNICAL TRANSLATIONS: Information published in a foreign language considered to merit NASA distribution in English.

SPECIAL PUBLICATIONS: Information derived from or of value to NASA activities. Publications include final reports of major projects, monographs, data compilations, handbooks, sourcebooks, and special bibliographies.

TECHNOLOGY UTILIZATION PUBLICATIONS: Information on technology used by NASA that may be of particular interest in commercial and other non-aerospace applications. Publications include Tech Briefs, Technology Utilization Reports and Technology Surveys.

Details on the availability of these publications may be obtained from:

SCIENTIFIC AND TECHNICAL INFORMATION OFFICE

NATIONAL AERONAUTICS AND SPACE ADMINISTRATION

Washington, D.C. 20546